STUDIES ON EXTRUSION – BASED ADDITIVE MANUFACTURING OF POLY-ETHER-ETHER-KETONE (PEEK)

R Mahesh Varma

A Dissertation Submitted to

Indian Institute of Technology Hyderabad

In Partial Fulfillment of the Requirements for
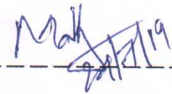
The Degree of Master of Technology

भारतीय प्रौद्योगिकी संस्थान हैदराबाद

Indian Institute of Technology Hyderabad

Department of Mechanical and Aerospace Engineering

June 2019

Declaration

I declare that this written submission represents my ideas in my own words, and where others' ideas or words have been included, I have adequately cited and referenced the original sources. I also declare that I have adhered to all principles of academic honesty and integrity and have not misrepresented or fabricated or falsified any idea/data/fact/source in my submission. I understand that any violation of the above will be a cause for disciplinary action by the Institute and can also evoke penal action from the sources that have thus not been properly cited, or from whom proper permission has not been taken when needed.
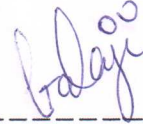
_____
(Signature)

_____
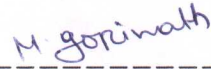R Mahesh Varma

_____
ME17AMTECH11013

Approval Sheet

This thesis entitled Studies on Extrusion-based Additive Manufacturing of Poly-ether-ether-ketone (PEEK) by R Mahesh Varma is approved for the degree of Master of Technology from IIT Hyderabad.

_____
Dr. Balaji Iyer (Examiner)

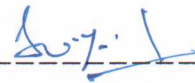Department of Chemical Engineering

_____
Dr. Gopinath Muvvala (Examiner)

Department of Aerospace and Mechanical Engineering

_____
Prof. N.Venkata Reddy (Advisor)

Department of Aerospace and Mechanical Engineering

_____
Dr. S.Suryakumar (Advisor)

Department of Aerospace and Mechanical Engineering

Acknowledgements

Dedication

Dedicated to my Parents and Friends

Abstract

Additive Manufacturing (AM) is a commonly used process in delivering complex parts with less lead time due to the absence of part specific tooling making it even economical for producing physical models or prototypes. Among all the AM processes, Fused Deposition Modeling (FDM) shares a huge fraction in application perspective for its relatively low equipment cost and ease of use.

The most commonly used materials for the FDM process include Acrylonitrile-Butadiene-Styrene (ABS) thermoplastics. Relatively new materials are being added to the list. One such material, which has been identified for its high performance and inert nature is Poly Ether Ether Ketone (PEEK). Its unique properties in delivering high service temperature and biocompatibility enhanced its application in Bio-medical and Aerospace industries. The higher melting temperature of PEEK makes it difficult to fabricate through FDM process. To address the challenge, Screw Extrusion process is employed due to its robust nature in handling materials.

The present work deals with processing PEEK material and fabricates components using principles of the AM process. The present study is mainly focused on important parameters like extrusion temperature, road width, standoff distance and print orientation in analyzing the mechanical behavior of PEEK samples. Experimental results suggest that extrusion temperature has a significant role in deciding the material characteristics. Extruding the PEEK above 350 $^\circ$C has degraded the material which resulted in losing materials properties. Also depositions made with lower road width settings has resulted in maximum interbond strength due to the better overlap of each deposition, thereby providing greater cross-section area when subjected to loading. Although experimental studies of tensile samples have been restricted to a single layer depositions, these can provide necessary understanding for multi-layer depositions.

Contents

List of figures

List of Tables

Nomenclature

D_b	Barrel inner diameter
H/d_c	Channel depth
w_f	Width of flange
δ_f	Clearance between barrel and tip of flange
ϕ	Helix angle
s	Screw lead
N	Screw rpm
$W_l(z)$	Melt fraction as a function of screw length
ρ_m	Density of melt
k_m	Thermal conductivity of melt
T_b	Surface temperature of barrel
T_m	Melting temperature of polymer
T_s	Surrounding/Ambient temperature
n_f	Melt flow efficiency
C_P	Specific Heat
H_m	Heat of fusion
W	Distance between flanges
X	Fraction of solid between flanges
F	Force acting on element

Abbreviations

AM   Additive Manufacturing

LOM   Laminated Object Manufacturing

FDM   Fused Deposition Modeling

SEM   Scanning Electron Microscope

SLA   Stereo Lithography

SLS   Selective Laser Sintering

PEEK   Poly-Ether-Ether-Ketone

PLA   Poly-Lactic-Acid

ABS   Acrylonitrile-Butadiene-Styrene

PC   Poly Carbonate

CHAPTER-1

Introduction and Literature review

1.1 Introduction

Additive Manufacturing (AM) is a manufacturing process in which a 3-D object is fabricated by adding material layer by layer. The input to AM is a 3D CAD file which is sliced into layers, and each layer is deposited. AM process converts raw material into a series of solid primitives in a layer by layer manner to obtain the desired component. The output is the fabrication of the component in a bottom-up fashion. Since this process can generate parts directly from CAD data file and does not require any setup or part specific tooling, it proves to be economical to make physical models or prototypes. AM process is used in many industries, but a major contribution is towards automotive, biomedical and aerospace industries for prototyping and some end-use applications. Although the basic process remains the same, the AM processes are broadly classified, as shown in Figure 1-1.
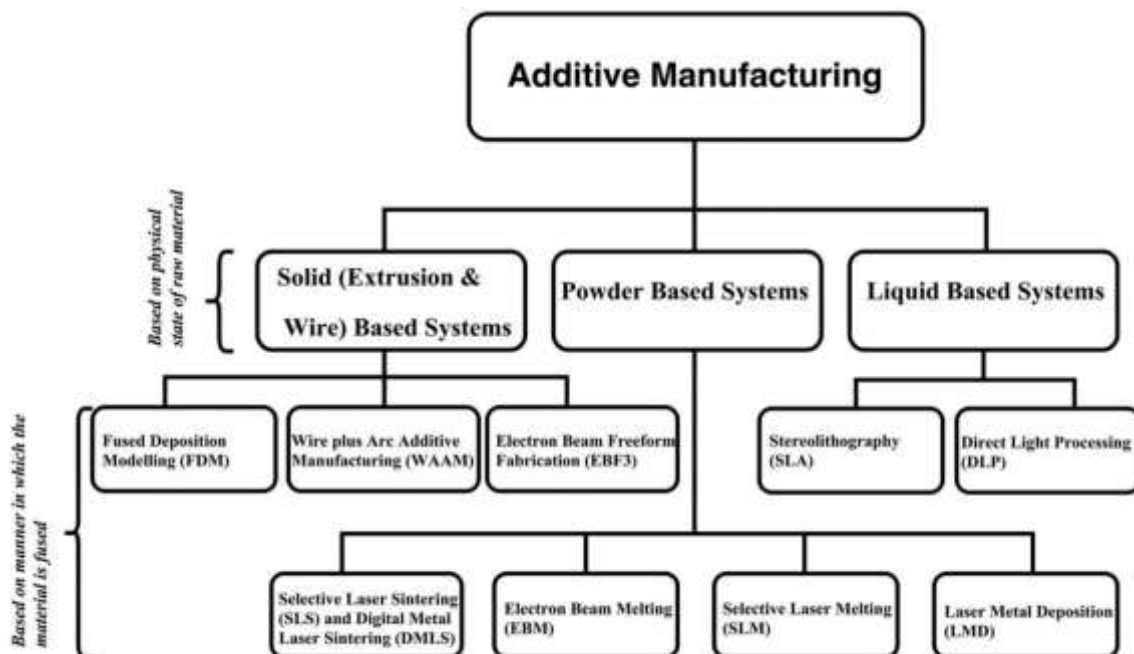
Figure 1-1 Classification of AM processes [1]

1.2   Fused Deposition Modeling (FDM)

In the FDM process, the thermoplastic wire is extruded through a heated nozzle. The heated material is deposited layer by layer to generate the required shape of the object. Setup of FDM is shown in Figure 1-2, which consists of XY table, wire filament, extruder with a heated nozzle. The raw material is generally available in the form of spool whose wire diameters generally is 1.75mm or 3mm of which 1.75mm is the most widely used. The wire is drawn from the spool with the help of driving wheels or rollers which are driven by a motor whose rotation speed depends on the printing speeds. As the wire enters the liquefier zone, it is heated so that the material is partially melted. In some cases, two materials are used simultaneously one for the component and the other for supporting overhangs in the component. Computer controlled positioning system is used to deposit the material according to the geometric profile of the object. The table is lowered after the completion of each layer and printing of subsequent layers is done in the same manner to create the final geometry. In most of the applications, the deposition process is performed in a closed environment with a suitable chamber temperature to provide proper printing environment. Once the final geometry is created the product or component is removed from the build platform and is subjected to post-processing if necessary.
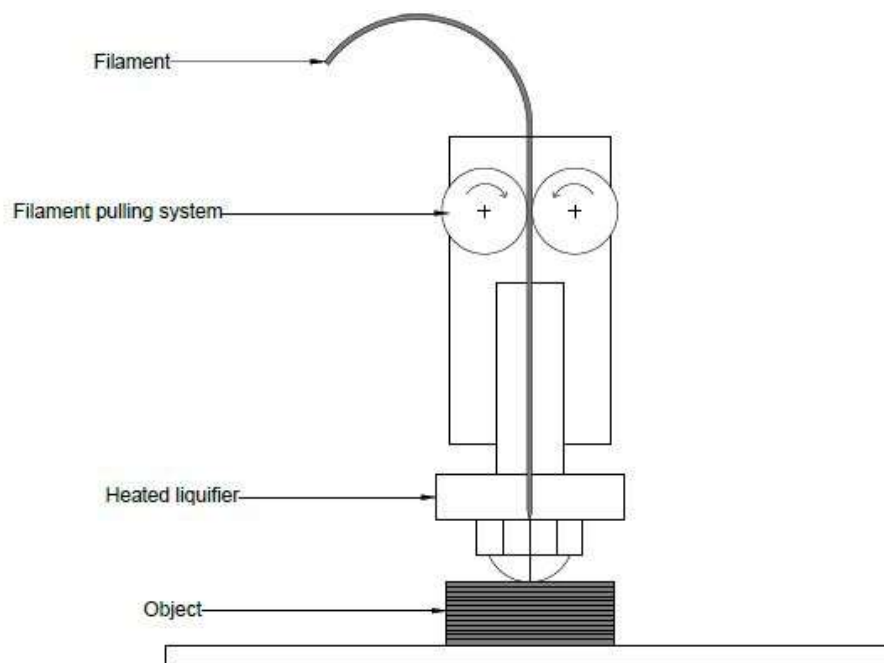
Figure 1- 2 Setup of Fused Deposition Modelling

1.2.1 Materials used in the FDM process

The most commonly used material for FDM is Acrylonitrile-Butadiene-Styrene(ABS). Components made with this process provide functional prototypes which are sometimes making way to end use applications. Since thermoplastic materials are environmentally stable and don't interact with ambient conditions with time, they are dimensionally accurate. Apart from ABS Polylactic Acid (PLA) and Polycarbonate (PC) are also widely used. With the desire for better mechanical properties, new materials have been identified for applications in the FDM process, which include Carbon Fiber reinforced composites and Poly Ether group [2].

1.2.2 Poly-Ether-Ether-Ketone (PEEK)

PEEK is among the most widely used high-performance semicrystalline thermoplastic polymer which originates from Poly Ether group. It has excellent mechanical, thermal and wear-resistant properties which make it very ideal for aerospace and automotive applications. It has the unique property of being inert, and its bio-compatibility has further widened its applications to medical fields for various bone implants. It is also flame retardant and good resistance to acids and alkalis, making it compatible even for chemically active environments. Properties for PEEK material are presented in Table 1-1 shown below

Table 1-1 PEEK properties [3]

Mechanical Properties	
Elastic Modulus	3.6 GPa
Poisson's ratio	0.38
Density	1310 Kg/m^3
Tensile Strength	95MPa
Compressive strength	125 MPa
Maximum crystallinity	43%
Thermal Properties	
Melting temperature	343 ˚C
Glass transition temperature	143 ˚C
Specific heat capacity	0.32 J/g-K
Thermal Conductivity	0.24 W/m-K
Flow Properties	
Melt Viscosity	350 Pa-s

1.2.3   Applications of FDM

The applications of 3D printed objects have grown to multiple fields, mainly due to its advantages. Parts produced by FDM process are most commonly used in medical, aerospace and automobile industries [2].

1.2.4   Advantages and limitations of the FDM process

Reasons for FDM being relatively more successful compared to other AM processes is due to its low cost and ease of use. Compared to other 3D printing processes such as Stereo Lithography Apparatus (SLA) which uses high energy laser for solidifying the photo resin, FDM process uses a heated nozzle to extrude material, which makes it much highly economical.

Although there are numerous benefits of the FDM process, it has certain limitations. The foremost one is that it can process materials which are available in spool or wire form only. Since a limited number of materials are available in the wire form to process through FDM, there is lesser material freedom to choose from. Although surface roughness can be improved by machining at the later stages, it still remains as a concern.

1.3   Screw Extrusion Process

Screw extrusion is a plastic processing method in which material is pressurized and forced through a die or a nozzle to get the required shape. This is one of the most widely used method for processing thermoplastic materials. The process consists of softening the material which is commonly known as plasticization or thermal softening after which it is extruded through an opening.

1.3.1   Setup

The basic components of a screw extruder include:

1. The screw which drives the material.
2. The barrel which confines the material
3. Nozzle which acts as a material exit.
4. Heating elements to supply external heat energy for softening of the polymer.
5. Motor for rotating the screw.

Schematic of a screw extruder is shown in Figure 1-3.
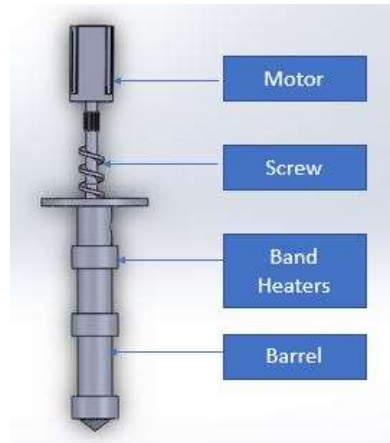
Figure 1- 3 Schematic of screw extruder setup

1.3.2   Various zones of the screw

Along the length of the screw, there are 3-zones through which the material passes before it gets extruded in the form of wire. Fig 1-4 shows the zones present, which includes the following.
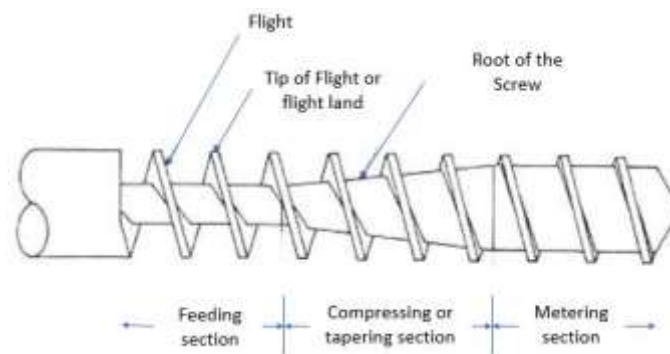
Figure 1- 4 Various zones of screw   [4]

1. Feeding zone is the primary zone which feeds the raw material to the upcoming zones. The channel depth in this zone is higher to accommodate more material. The material is fed into this zone using gravity through the feeding pipe, from hopper. The feeding pipe is usually non-metallic to avoid heat to be transferred, which causes pre-melting of pellet and thereby clogging the passage.

2. Compression zone compresses the material and viscous shearing of the material generates necessary heat to soften the polymer. Along the compression zone, the diameter of the screw increases towards the exit for providing the necessary

5

compression. The ratio of diameters at the beginning and end of the compression zone is called as compression ratio and varies depending on the polymer that is being processed. The length of the compression zone depends on the polymer that is being processed, i.e. semi-crystalline or amorphous nature. Although external heating is supplied by band heaters. Majority of the heat is produced because of the viscous shearing that happens during compression. The mechanism of viscous shearing is explained in Figure 1-5.
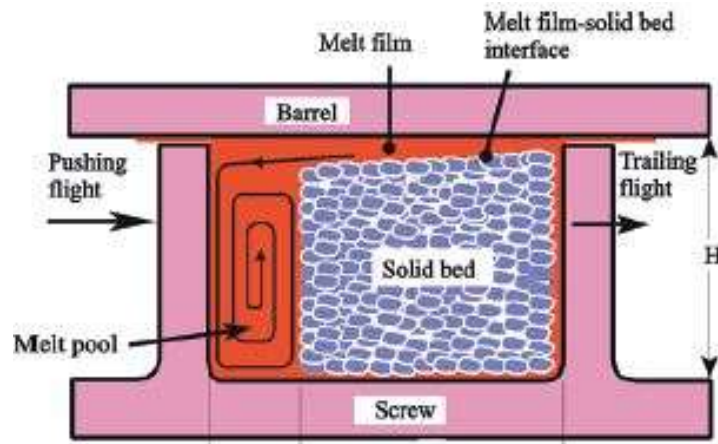
Figure 1- 5 Viscous shearing mechanism   [5]

As the material moves between the flanges of the screw, the solid bed is sheared with viscous melt producing friction between the interfaces. This results in softening of the solid material and eventually converting it to melt. This process continues till the solid material between the flanges is converted to the melt. Usually, the compression zone is designed in such a way that by the time the material comes towards the end, all the solid material is converted into the melt. The third zone includes a metering zone, which ensures proper mixing of material and generating appropriate pressure to overcome the back pressure and transport the material towards the nozzle exit. The material comes out of the nozzle in the form of wire which is ready to solidify and takes the desired shape.

1.4   Literature review

Many researchers made attempts to understand the influence of temperature and extrusion parameters to 3-D print PEEK material. Some of their findings based on experimental studies are presented below.

1.4.1   Parameter study of 3-D Printed PEEK parts

Rinaldi et al. [6] has conducted experiments on additive manufacturing of PEEK using fused deposition modelling to understand mechanical, thermal, microstructure and morphological aspects. Parameters considered included print orientation and infill ratios. Figure 1-6 shows print orientation used in their experiments.
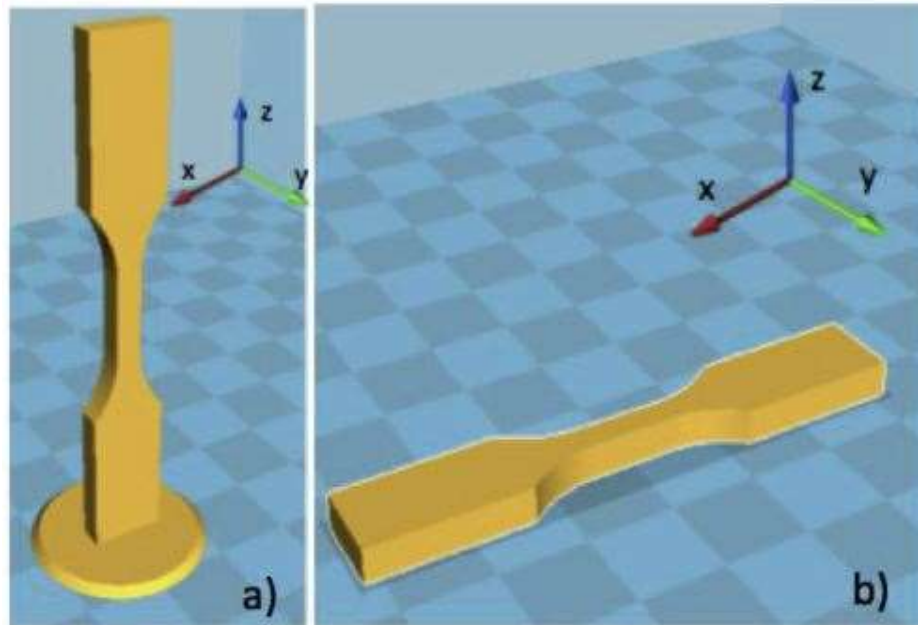
Figure 1- 6 Orientation of printed parts a) Along Z- direction b) Along X-Y direction   [6]

They concluded that infill ratio and deposition pattern have considerable influence on the mechanical properties. Parts with a higher infill ratio had more material to resist load, which improved their tensile strength. Figure 1-7 shows stress-strain plots for parts printed in XY and Z orientations with infill ratios corresponding to 100%, 50% and 20%.
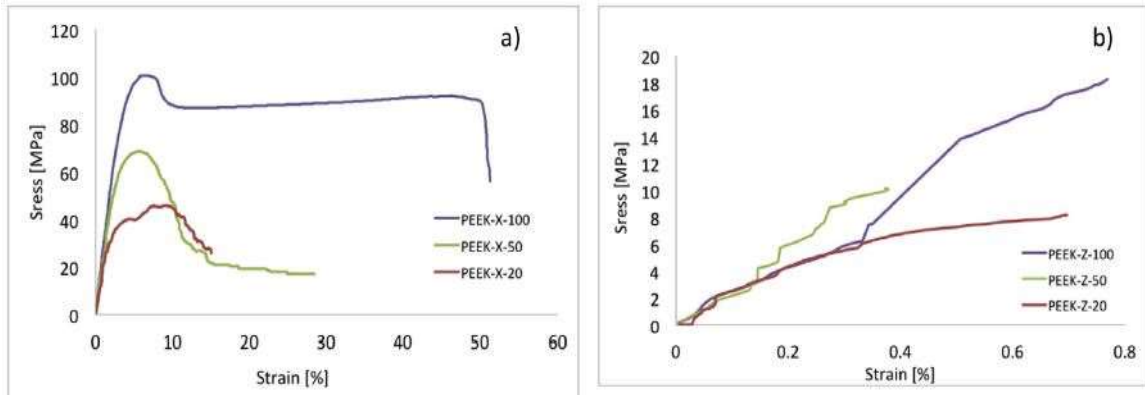
Figure 1- 7 Stress-strain curve for parts printed with infill ratio 100%,50%,20%

a) Along XY direction b) Along Z direction   [6]

They reported that the samples printed along XY direction had shown appreciable deformation along the direction of loading, while the samples printed in Z direction has failed in a brittle manner primarily due to adhesive failure between layers. Based on the mechanism of failure, it was concluded that samples printed with XY direction have higher strength than samples printed along the Z direction. Figure 1-8 shown below describes the mode of failure for each printing orientation respectively.
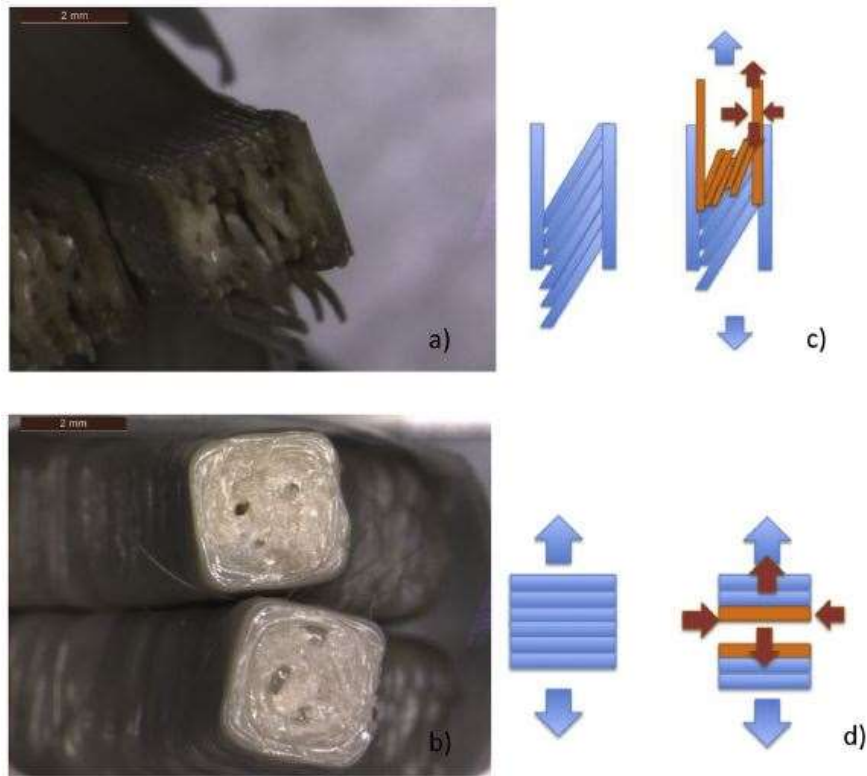
Figure 1- 8 Fracture after tensile test a), b) XY direction printed samples

c), d) Z direction printed samples   [6]

8

Deng et al. [7] studied the effects of printing speeds, layer thickness, printing temperature and filling ratio on tensile properties. Table 1-2 shows the parameter and their levels used to perform experiments.

Table 1-2 Printing parameters   [7]

Level	Factor			
	Printing Speed (mm/s) A	Layer Thickness (mm) B	Printing Temperature (°C) C	Filling Ratio (%) D
1	20	.20	350	20
2	40	.25	360	40
3	60	.30	370	60

Table 1-3 describes the orthogonal array used for conducting experiments and Figure 1-9 shows the variation of tensile strength for different parameter settings.

Table 1-3 Orthogonal array design   [7]

No	Factor			
	A	B	C	D
1	20	.20	350	20
2	20	.25	360	40
3	20	.30	370	60
4	40	.20	360	60
5	40	.25	370	20
6	40	.30	350	40
7	60	.20	370	40
8	60	.25	350	60
9	60	.30	360	20
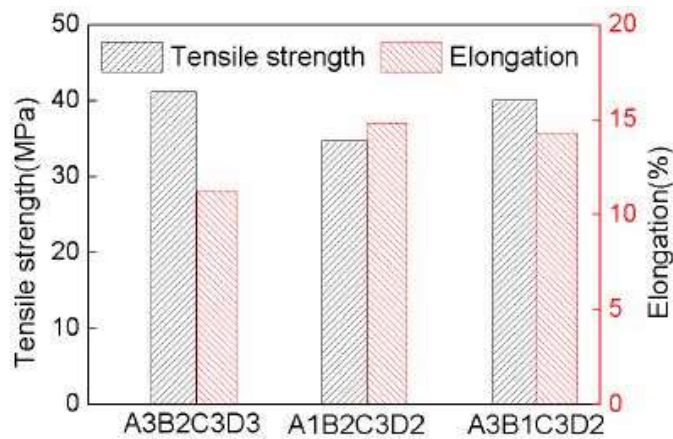
Figure 1- 9 Comparison of tensile properties for different printing parameters   [7]

It was reported that the primary reasons for fracture were due to layer thickness and infill ratio. It was also reported that the combination of low and high processing parameters had exerted poor mechanical properties. Also, layer thickness was identified to affect the width and

printing speed of filament, which has an impact on mechanical strength due to their bonding behaviour.

1.4.2   Comparison of PEEK with other thermoplastics

When compared to other thermoplastics, PEEK establishes itself as high-performance thermoplastic. Studies have been made to compare PEEK material with other commonly used thermoplastics. Xiaoyong et al. [8] have compared PEEK components with that of PLA by studying the effects of temperature control and infill ratio on bonding strength which influences the mechanical properties. It was reported from the experiments that bed temperature and ambient temperature has great influence on the mechanical properties of PEEK printed component. It was also reported that samples with higher bed and ambient temperature had enhanced PEEK binding forces between layers which contributed to a better tensile strength of 75MPa

Wenzheng et al. [9] conducted experiments to study the influence of layer thickness, and raster angle on mechanical properties of 3D printed PEEK parts and conducted a comparative analysis of mechanical properties for PEEK with ABS parts. They concluded that layer thickness has a significant impact on tensile, compressive and bending properties. Also, the comparison between PEEK and ABS indicated that PEEK samples showed 108% higher tensile strength compared to ABS and compressive strength of 114% higher than that of ABS material. Figure 1-10 and Figure 1-11 shows engineering stress Vs engineering strain plots for ABS and PEEK plastic during tensile and compressive loading respectively
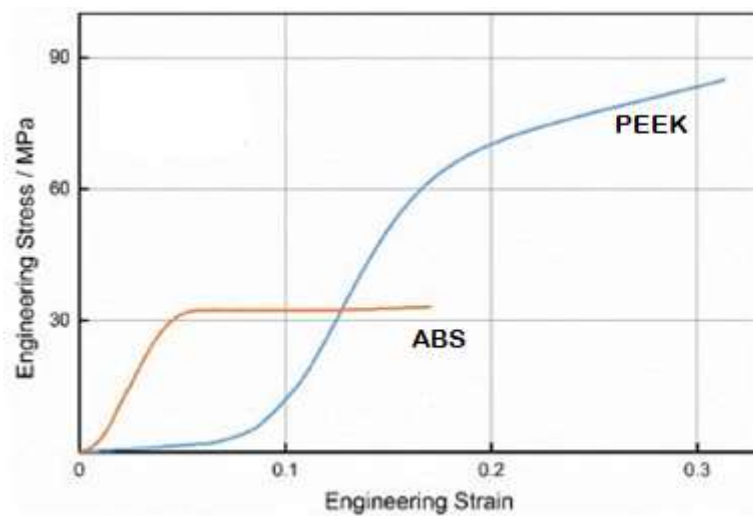
Figure 1- 10 Tensile stress-strain curve for ABS and PEEK   [9]
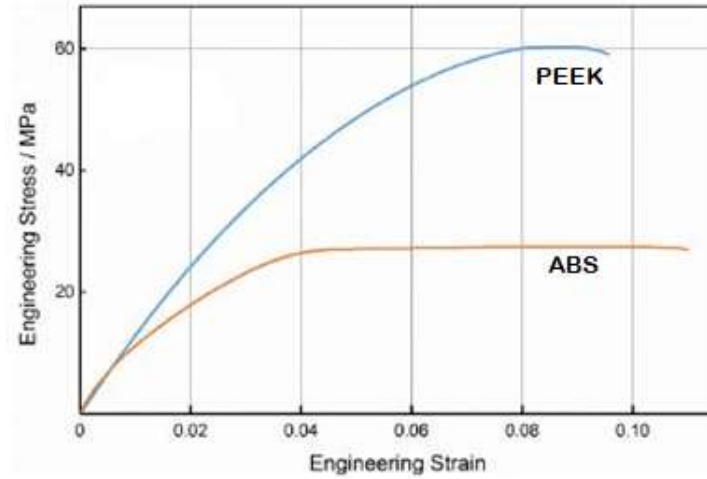
Figure 1- 11 Compressive stress-strain curve for ABS and PEEK   [9]

1.4.3   Study on temperature and crystallinity

Properties of thermoplastics are dependent on crystallinity. Hence proper thermal processing is important in maintaining the crystalline nature. Yang et al. [10] conducted experiments to find the influence of thermal processing conditions on crystallinity and mechanical properties of PEEK 3D printed samples. The study consisted of investigating the relations between ambient temperature, nozzle temperature and heat treatment methods. Figure 1-12 shows heat treatment methods used with their time-temperature plot.
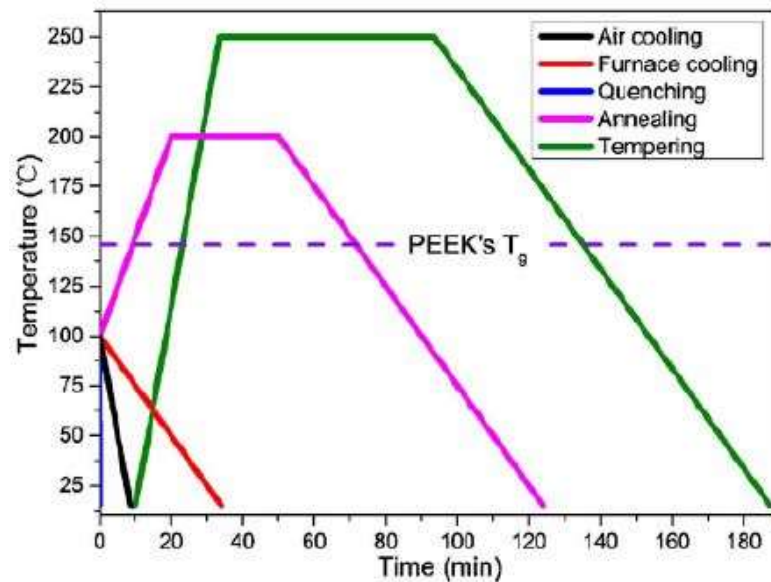
Figure 1- 12 Time temperature description in different heat treatment methods   [10]

It has been reported that samples which have undergone annealing and furnace cooling have yielded better crystallinity, thereby improving their mechanical properties. This was due

to slow cooling which allowed material to achieve maximum crystallinity. Figure 1-13 shows the graphical representation of crystallinity and breaking elongation obtained for different heat treatment methods. Also, it was reported that higher ambient temperature has shown better properties, which is contributed due to higher energy and time for improving crystallinity.
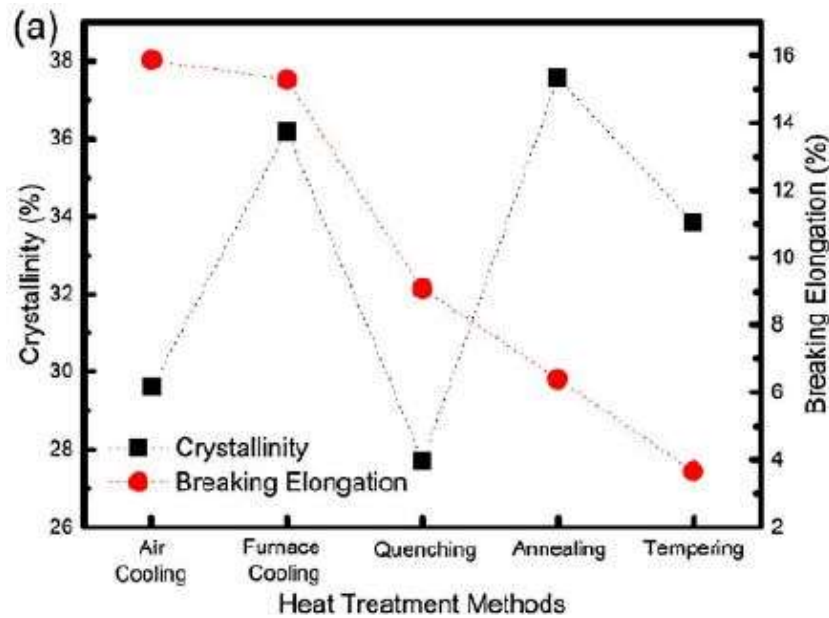
Figure 1- 13 Crystallinity and breaking elongation for different heat treatment methods   [10]

Eduljee et al. [12] have studied how residual stresses are developed in PEEK material and proposed a residual stress model with a combination of material properties to identify the effects of crystallization mechanism in semi-crystalline materials. From their models, it was reported that rapid cooling has suppressed the crystallization of PEEK. It was also reported that sufficient slow cooling reduced the temperature gradients, thereby giving enough time for PEEK to crystallize. In their model, no relation between residual stress and shrinkage due to crystallization have been identified.

1.4.4   Extrusion process

Attempts have been made to fabricate parts through screw extrusion process. Bellini et al. [15] have developed an extruder setup as an alternative to the FDM process to fabricate components. This was done by mounting mini extruder on a high precision positioning system that can operate with bulk materials in granulated form. Although the process was successful in depositing samples, problems related to air entrapments is prominent. This was primarily

due to uniform channel depth in his screw along with the rotational history in the material. Figure 1-14 shows setup developed and screw used for processing
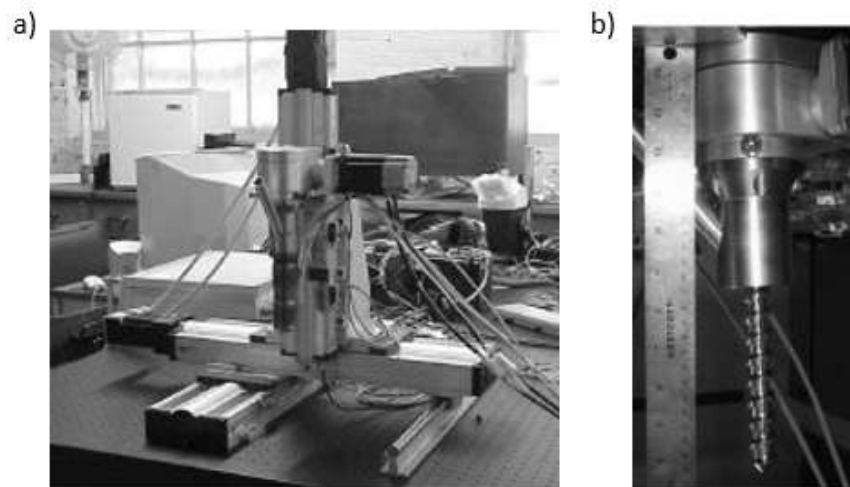
Figure 1-14 a) Mini Extruder Setup b) Screw profile   [15]

Based on the limitations of Bellini et al [15] Reddy et al. [17] has developed screw extruder setup with screw design by facilitating varying channel depth (tapered screw design) and spider bearing. As shown in Figure 1-15, the spider bearing consists of a disc with circular holes that was inserted in the adapter to reduce the effect of rotational history in the polymer by breaking the flow. This ensured that the flow was uniform and continuous with minimal air entrapments. Later experimental studies were conducted on ABS thermoplastic using the screw extrusion setup to study its mechanical behaviour by varying process parameters, which include nozzle temperature, chamber temperature and road width. It was reported that higher nozzle temperature and lower road gap has resulted in better surface finish while chamber temperature had little effect on surface finish.

Figure 1-15 Spider bearing used in extruder setup   [17]

13

Drotman et al. [18] have developed screw extrusion-based additive manufacturing setup for Poly Lactic Acid (PLA) material. The process consisted of designing the screw with the appropriate L/D ratio of 18:1 to suite material requirements. Figure 1-16 shows a schematic of the setup used for fabricating PLA filament. Material flow rate and back pressure have been calculated along with studies on the interaction of material flow with screw speed for uninterrupted flow of material through the nozzle during the deposition process. It was reported that higher nozzle temperatures and screw speed resulted in maximum material flow overcoming the back pressure which resulted in a continuous flow of material.
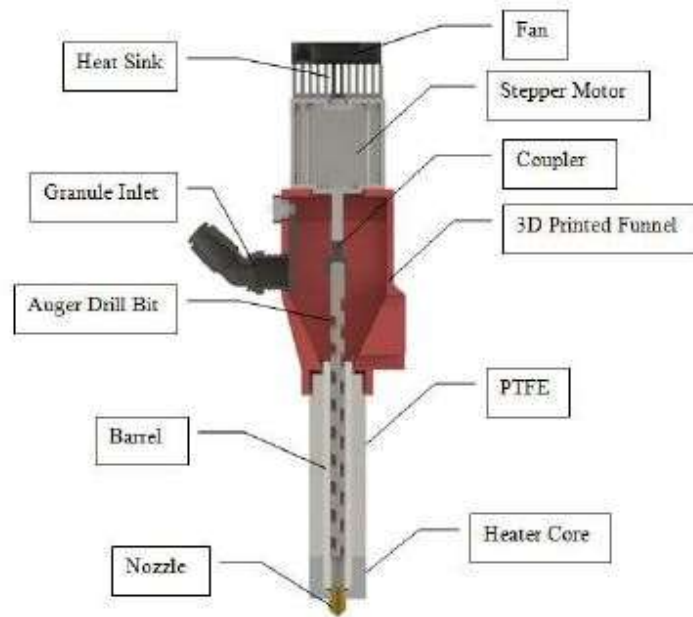
Figure 1- 16 Schematic of setup used for fabricating PLA filament.   [18]

Tseng et al. [19] have designed a 3D printing system which is based on screw extrusion for PEEK material to overcome the limitation of the filament feeding system. Experiments were conducted to study the effects of print direction, nozzle temperature, bed temperature and annealing process on tensile strength of printed samples. Figure 1-17 shows the variation of tensile strength for different parameter setting. It was reported that nozzle temperature in the range of $370\,^\circ$C -$390\,^\circ$C and bed temperature of $280\,^\circ$C along with the print direction of $0\,^\circ$ has resulted in maximum tensile strength. It was also reported that the annealing process did not provide any improvement in the mechanical properties of the samples.
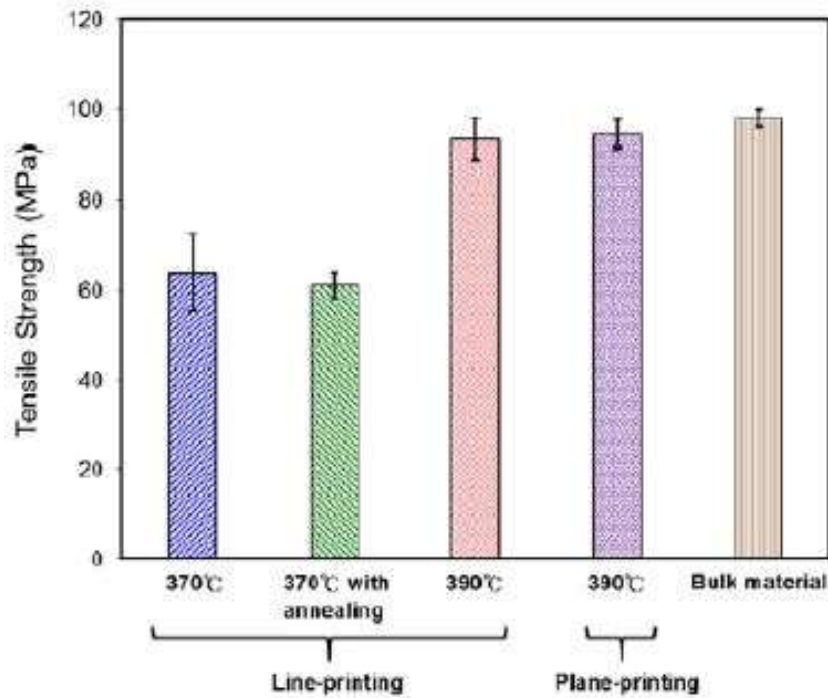
Figure 1-17 Tensile strength of PEEK samples for different print direction and

temperature setting   [19]

Termoplasti et al. [20] have developed a PEEK extrusion setup which used the rod as raw material to convert it into wire form by extruding it through a small nozzle. Experiments were conducted to study the mechanical properties of deposited samples. SEM results as shown in Figure 1-18 revealed the presence of air entrapments due to the presence of moisture content which resulted in the lowering of tensile strength for deposited samples.
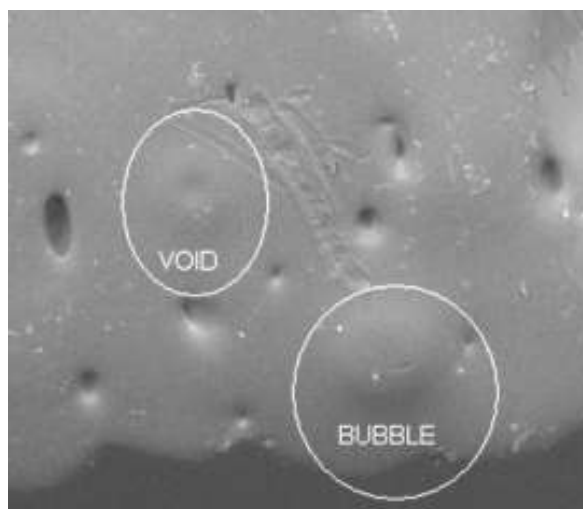
Figure 1-18 Voids and Bubbles formed in PEEK samples due to moisture content

[20]

Whyman et al. [21] developed pellet-based extrusion system for printing bio-polymers and studied the effects of various printing parameters, which include nozzle size, print speed and layer thickness. Figure 1-19 describes the setup that was used for 3-D printing of PLA material.
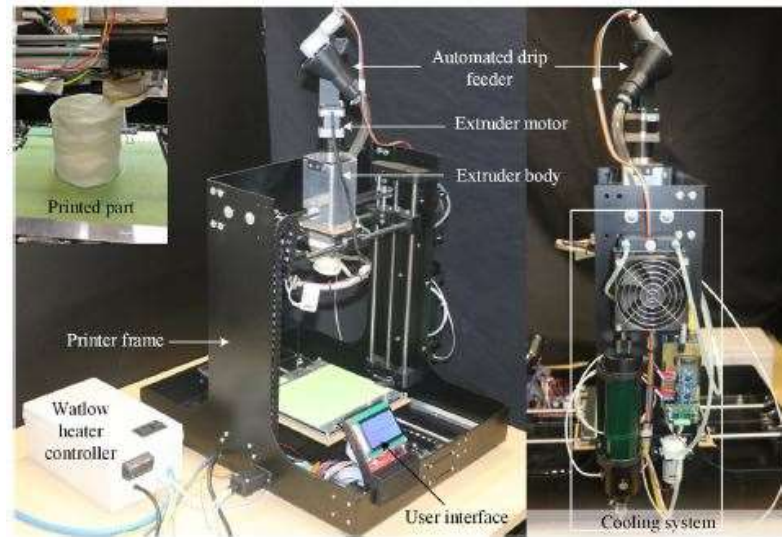
Figure 1- 19 Setup used for 3-d printing of PLA   [21]

It was reported that samples deposited with lower print speeds and higher nozzle temperature have resulted in higher tensile strength. It was also reported that specimen deposited with higher print speeds and small nozzle size had voids as shown in Figure 1-20, which resulted in weak strength of the specimen. Also, problems encountered during the printing process as shown in Figure 1-21, which include improper filling, inconsistent bonding and material clogging in the screw were reported.
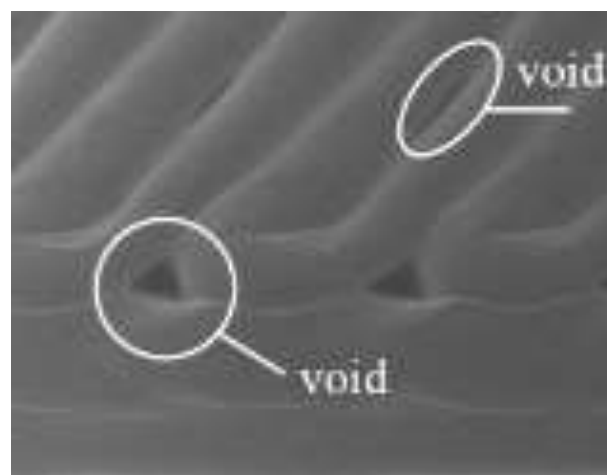
Figure 1-20 Topographical image which shows voids in deposited samples [21]
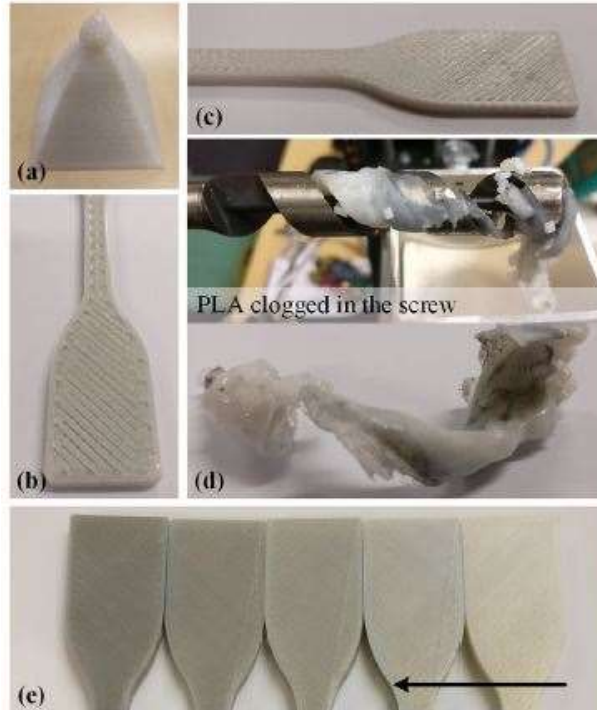
Figure 1- 21 Problems found during the course of development and optimization of the extrusion system. a) Lack of rapid layer cooling resulted in a material blob, b) improper filling, c) inconsistent bonding on the build surface, d) material clogging in the screw, and e) colour change due to contamination from the extruder walls   [21]

1.5   Objectives

The objectives of the current study include the following:

1. To perform thermal analysis and estimate temperature profile variation with time for extruding PEEK material with the existing setup.

2. To study the influence of thermal processing parameters on PEEK extruded samples.

3. To measure tensile strength as well as inter road bond strength of extruded material.

CHAPTER-2

Finite Element Modeling of Screw Extrusion process

2.1 Introduction

This chapter discusses on Finite Element Modeling of extrusion process for PEEK material based on screw-barrel geometry and material properties. Transient thermal analysis is performed to estimate the variation of temperature profile with time and the time required for the process to reach steady-state conditions. During the modelling, the following assumptions are considered, which are listed below.

1. The thermal and physical properties of the material are considered to be independent of temperature variation.
2. Heat is being conducted only radially into the barrel.
3. No thermal contact resistance is considered at the interface.

2.2 Geometric model and material properties

The geometric parameters of the screw-barrel components that have been used to model are mentioned in Fig 2-1 and described in Table 2-1.
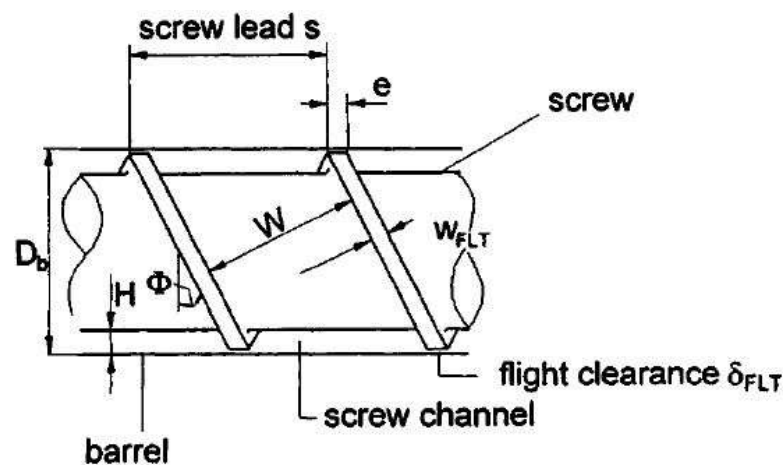
Figure 2 - 1 Nomenclature of screw extruder   [14]

18

Table 2-1 Screw-Barrel geometric parameters   [14]

Parameter	Description	Magnitude
D_i	Barrel diameter	30 mm
D_o	Barrel outer diameter	50 mm
H	Channel depth	6 mm
w_f	Width of flange	5 mm
δ_f	Clearance between barrel and tip of the flange	0.2 mm
ϕ	Helix angle	17.66˚
s	Screw lead	23.8 mm
L	Total screw length	240 mm

The screw extruder setup includes components with different materials for barrel, screw and adapter whose properties have been listed in Table 2-2.

Table 2-2 Material properties data used for performing numerical analysis

Material/ Property	Brass (Adapter)		PEEK (Polymer)		EN 8 steel (Barrel and Screw)	
Conductivity	110	W/m-K	.24	W/m-K	40	W/m-K
Density	8550	Kg/m^3	1310	Kg/m^3	7800	Kg/m^3
Specific heat	.39	J/g-K	.33	J/g-K	.50	J/g-K

2.3   Thermal analysis of Screw Extrusion

Thermal analysis of screw extruder was performed to study energy balance for the control volume and propose boundary conditions by identifying the forms of energy transfer that takes place between the system and surroundings. Energy for the screw extrusion system is basically supplied in two forms, one in the form of thermal energy (by heating the surface of the barrel using band heaters), and other in the form of mechanical energy (for rotating the screw using the motor). The thermal energy supplied by the band heaters will play a major role in converting solid material to semi-solid melt and a large fraction of mechanical energy is converted into heat by viscous shearing effect, while a small portion of it is consumed in generating melt pressure as the material proceeds towards the exit. The utilization of the total thermal energy (heat from band heaters and heat generated due to the viscous shearing effect)

in the system is analyzed by partitioning the extrusion system into different zones. The heat transfer modes in different zones have been represented in Figure 2-2. The heat flows from band heaters to the first, third and fifth zones by conduction, while the heat losses in remaining zones primarily take place by convection.
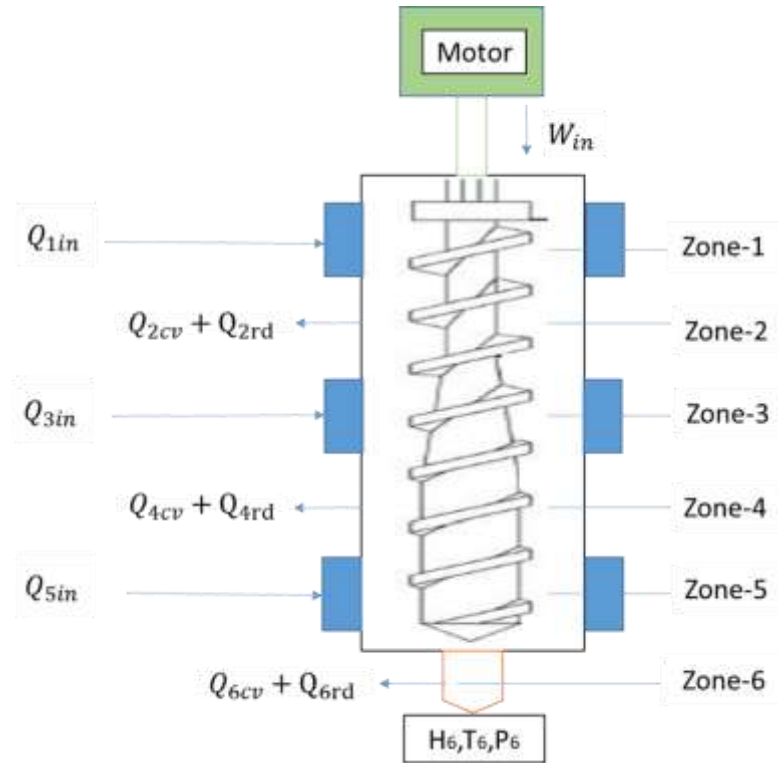
Figure 2-2 Schematic of energy balance in a screw extruder

The material enters into the system with temperature T1, i.e. room temperature and pressure P1 atmospheric pressure and enthalpy H1. As the material moves forward its pressure temperature and enthalpy change to P6 T6 and H6 at the exit of the nozzle. The heat energy (Q) supplied to the system is considered as positive while the heat energy lost by the system is considered as negative. Similarly work done (W) on the system is considered negative while work done on the system is considered positive. Hence energy balance for control volume analysis can be written as

$$\Delta H + \Delta PE + \Delta KE = \Delta Q - \Delta W \qquad (1)$$

Where

ΔH Indicates the change in enthalpy per unit mass of the polymer.

ΔPE Represents gain in potential energy of the polymer per unit mass as the material moves down towards the nozzle end.

ΔKE Indicates the kinetic energy involved in the polymer transfer per unit mass.

ΔQ Indicates the net thermal energy given to the polymer per unit masses

ΔW Indicates the net mechanical energy given to the polymer per unit mass

Since the effect of kinetic and potential energy terms are neglected in our system hence equation (1) reduces to

$$\Delta H = \Delta Q - \Delta W \tag{2}$$

The net thermal energy supplied to the system can be inferred from Figure 2-2 as

$$\Delta Q = Q_{1in} - (Q_{2cv} + Q_{2rd}) + Q_{3in} - (Q_{4cv} + Q_{4rd}) \tag{3}$$
$$+ Q_{5in} - (Q_{6cv} + Q_{6rd})$$

Substituting equation (3) in equation (2), the change in enthalpy in the system can be obtained as

$$\Delta H = Q_{1in} - (Q_{2cv} + Q_{2rd}) + Q_{3in} - (Q_{4cv} + Q_{4rd}) \tag{4}$$
$$+ Q_{5in} - (Q_{6cv} + Q_{6rd}) - \Delta W$$

2.4   Boundary Conditions and mesh generation

Axis symmetric model has been created using the Abaqus software to investigate the temperature profile at different locations in the extruder setup. Figure 2-3 describes the boundary conditions that have been considered. As previously mentioned, different zones, i.e. feeding section, compression section and metering section have been given temperatures of 250 °C, 315 °C and 340 °C respectively. The heat transfer to supporting components of the system has been considered negligible hence heat flux of magnitude zero has been assigned at contact regions between the barrel and supporting frame. The ambient temperature was assigned as 30 °C through predefined fields. As discussed from the energy balance of screw extrusion process, convection and radiation losses have been assigned at regions exposed to surroundings.
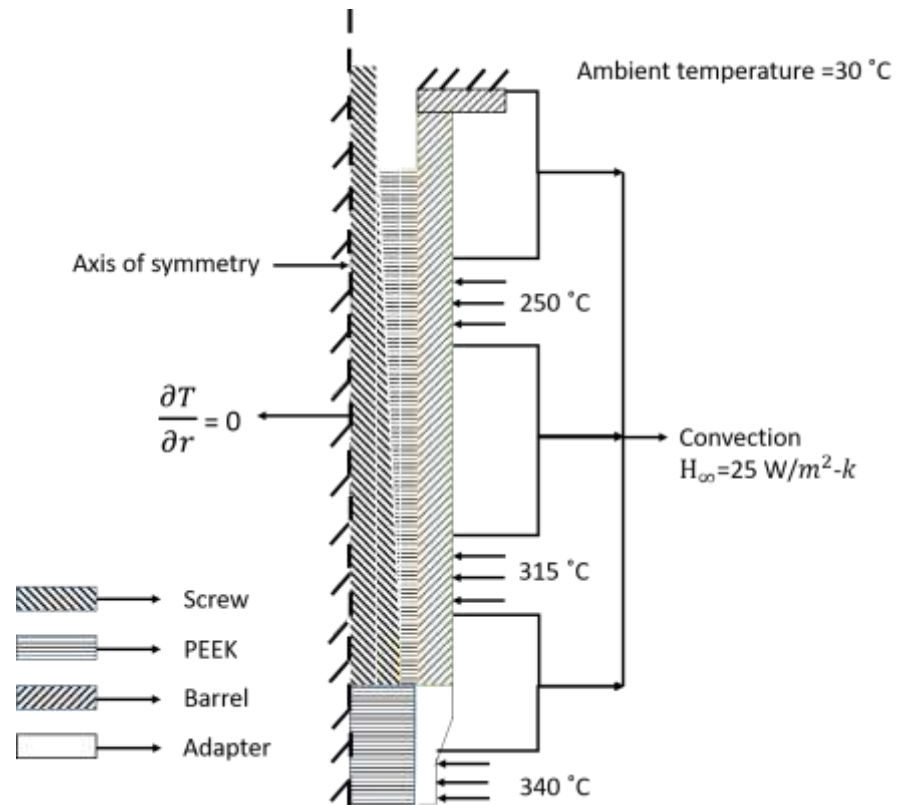
Figure 2-3 Boundary conditions used for studying temperature profiles

The numerical modeling is carried out based on axisymmetric transient thermal analysis, so corresponding mesh is generated using axisymmetric 4-noded quadrilateral convection- diffusion element (DCCAX4) with mesh size of 2.5 mm x 2.5 mm.

2.5   Results

Numerical modelling of the screw extrusion process was performed using transient thermal analysis to study the variation of temperature profiles with time. From results it was observed that after the temperature reaches the specified temperature on the outer surface of the barrel, the heat slowly transfers throughout the barrel surface in the lateral direction followed by heat flow in the radial direction as shown in Figure 2-4. This behaviour is possibly due to bad conductivity of polymer, which resists the heat flow to the inner section of the extruder. As time progresses, the heat transfer in the system reaches steady state and temperature stabilizes.
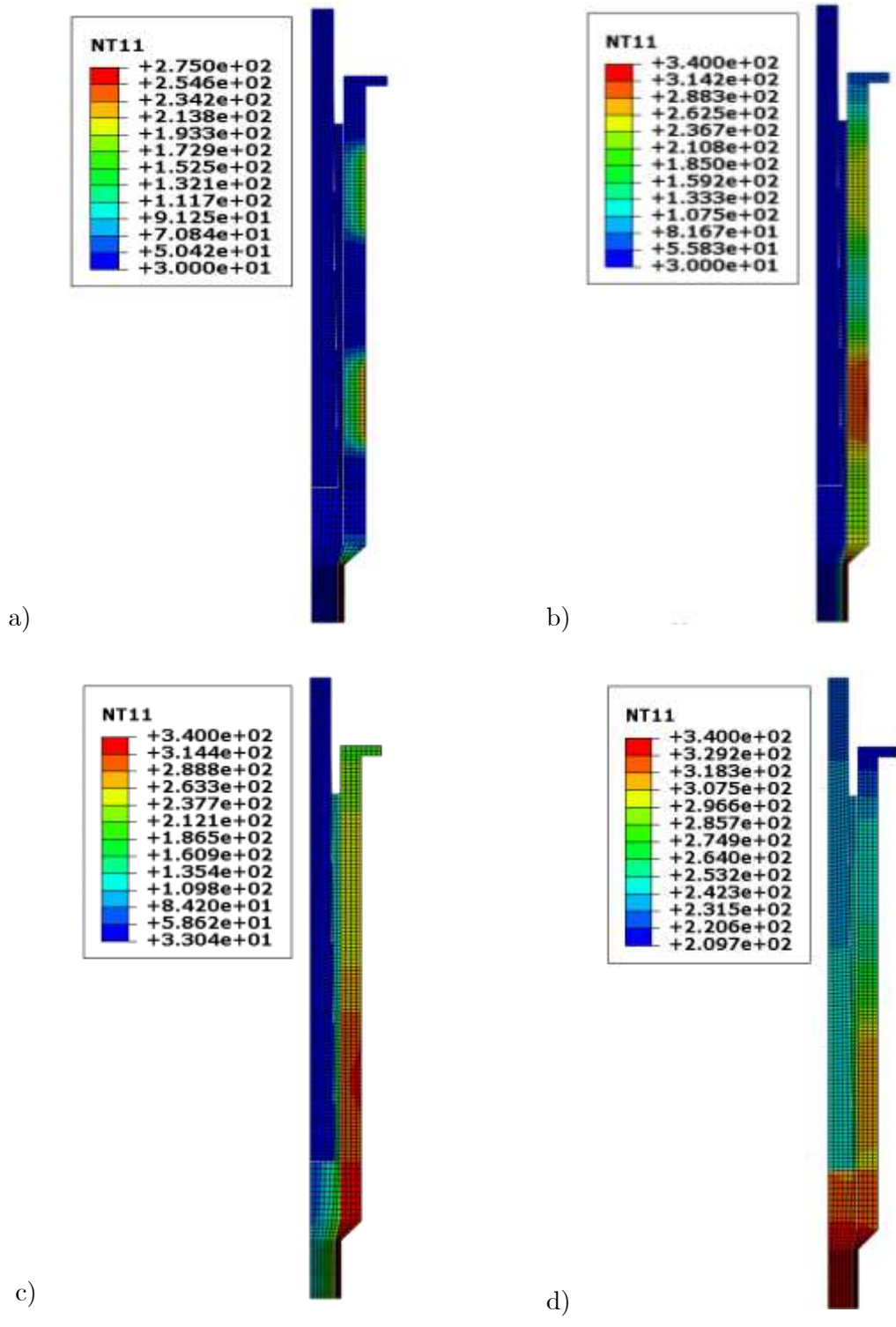
Figure 2-4 Temperature profile variation with time plots from Abaqus

a) 2 minutes b) 10 minutes c) 30 minutes d) 100 minutes

Temperature variation with respect to time for different nodal temperatures has revealed that the stabilization time varies based on location in the extruder setup, as shown in Figure 2-5.
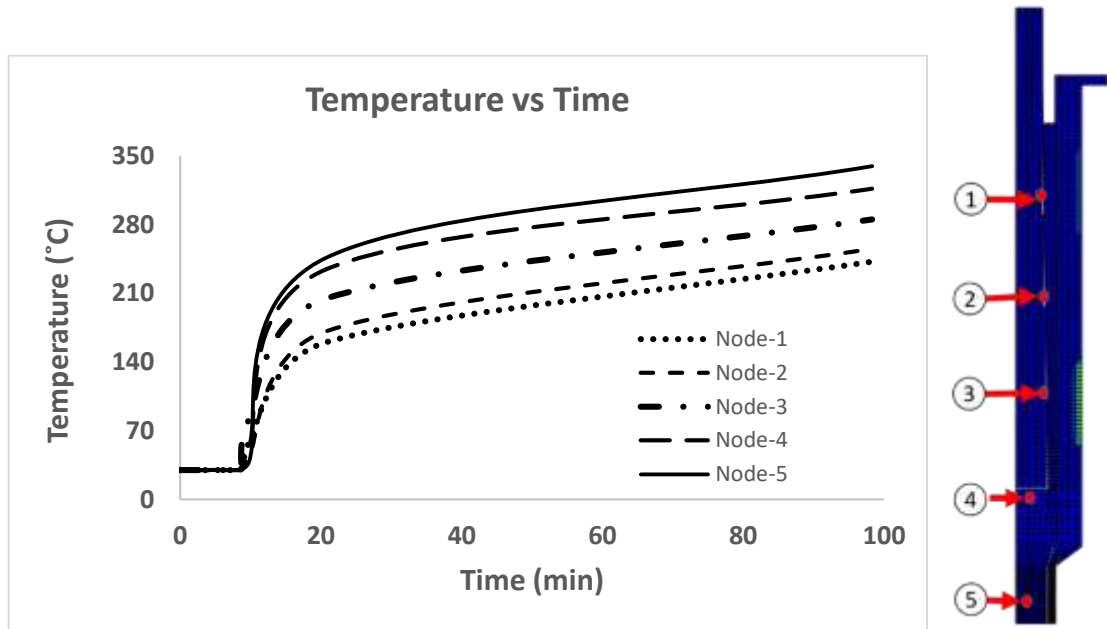
Figure 2-5 Temperature profile on selected nodes

In order to perform the experiments, the maximum stabilization time among all regions of the model was determined. From the numerical analysis, it was evident that the nodal location 5 has the maximum stabilization time of 90 minutes, as shown in Figure 2-5.

2.6 Summary and conclusion

Numerical simulation has been carried out by transient thermal analysis to study the temperature profile variations with respect to time for PEEK extrusion. Energy balance of the screw extruder has been discussed to describe the boundary conditions that are imposed on the system. It was identified from results that stabilization time of 90 minutes is required for the system to reach steady-state conditions before extruding the material from the extruder setup.

CHAPTER-3

Experimental Design

3.1 Introduction

This chapter discusses preliminary experiments on processing PEEK through setup that has been developed by Reddy et al. [14]. Also, experimental design is discussed to study mechanical characteristics for different process parameters. The preliminary aim of experimentation is to analyze how the tensile strength of the sample is being affected by varying parameters within a specified range. The basic components used for experiments include extrusion setup, which includes assembled components like band heaters, motor, gear arrangement and XY-table as shown in Figure 3-1 and Figure 3-2.

Figure 3-1 Setup used for experimentation

Figure 3-2 XY table

The XY-table is controlled through Arduino programming to maintain a precise movement. The controlling unit consists of hardware components, which include DC power supply for the motors and primary switches to execute the motion of each axis and the controllers for each axis. Table 3-1 discusses the mechanical specifications of the XY table setup. The speed control of the XY table and individual motor activation is done through programming inputs. The present XY table does not have any reference position, and after every cycle of the experiment, it has to be brought to the beginning position by manual control of individual axis, as shown in Figure 3-3.
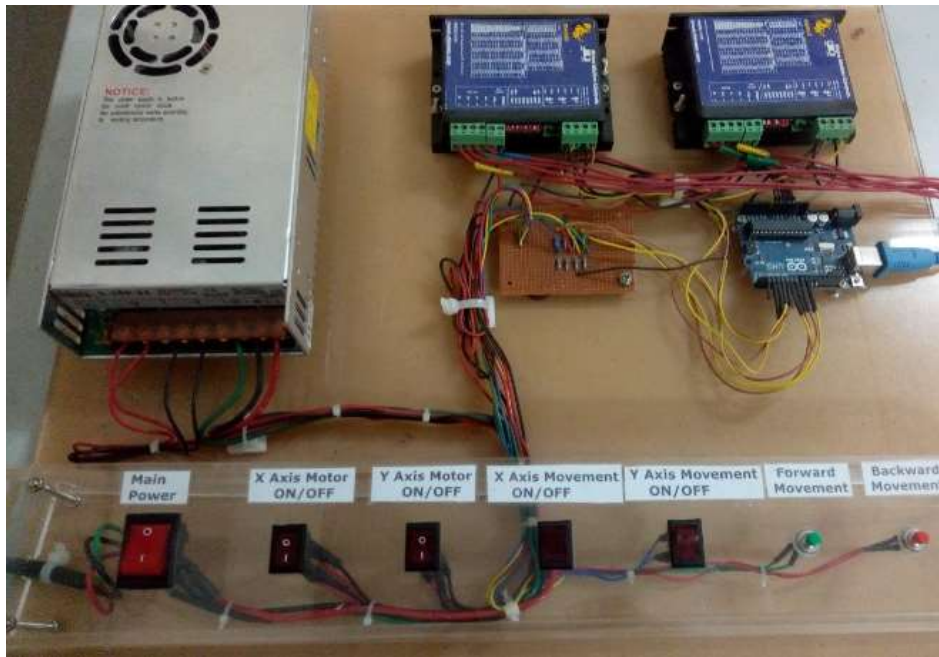
Figure 3-3 XY table controller unit

Table 3-1 Specifications of the XY table

Parameter	Magnitude
X-axis maximum displacement	100 mm
Y-axis maximum displacement	100 mm
Lead screw pitch	4 mm
Maximum speed for table movement	3mm/sec
Minimum speed for table movement	0.1mm/sec

The material in the pellet form moves from funnel through a feeding channel to the inlet provided on the barrel with the help of gravity. The feeding channel is provided with an arrangement to stop or start the feeding but it has to be noted that there is no specific control for material flow, hence manual intervention is required for feeding material. Through analytical calculation, the torque requirements for processing PEEK was estimated as 24.5 N-m, Hence DC-motor with a torque capacity of 10 N-m along with a gear ratio of 3:1 was chosen to provide net torque of 30 N-m for the screw. Since the melting temperature of PEEK was on the higher side hence ceramic band heaters with a working range of 100 °C to 450 °C has been chosen to perform experiments. Fig 3-4 shows ceramic band heaters assembled onto the barrel.

Figure 3-4 Ceramic heater used for experiments

3.2 Process parameters and response variables

The process parameters that have been considered for experimentation include

1. Nozzle size
2. Extrusion temperature
3. Road width
4. Print direction
5. Stand off distance

With the available group of process parameters and response variables two different sets of experiments were performed as listed below

1. To find the tensile strength of the PEEK wire sample
2. To estimate the bond strength of multi-pass samples

3.3 Preparation of wire samples

The major parameter of interest of PEEK extruded wire samples was to find out its Ultimate tensile strength and also temperature settings to facilitate optimal characteristics of the material. The governing parameters for wire testing included the following

1. Extrusion temperatures at different zones
2. Extrusion time after the steady-state temperature is reached.

3.3.1 Extrusion temperature

Among all the parameters available, extrusion temperature has a significant contribution in deciding the mechanical behaviour of samples. Higher extrusion temperature may cause unnecessary material degradation which results in material losing its characteristics, while too low extrusion temperature causes insufficient mixing causing discontinuous flow of material from the nozzle. Hence it is very important to choose appropriate extrusion temperature for experimentation. Since there are different sections along the screw and barrel section, each section has a certain range of temperatures to operate for extrusion to happen properly.

3.3.1.1 Feeding Zone

The initial region which corresponds to the feeding section is where the heat supply begins with band heaters. Of all the sections the feeding section needs to have the minimum temperature to allows the material, accept thermal energy slowly and gradually. The temperature of 220 °C was initially considered for feeding section with a continuous increase of 15 °C for every set of experiments. It has to be noted that using conduction principles, the net heat transfers into the barrel were estimated as 15 °C less than what was supplied on the surface.

3.3.1.2 Compression Zone

In the compression zone, two types of energies play important role. One in the form of mechanical to shear the material with the help of rotating screw and other in the form of

externally supplied heat energy to maintain temperature. Since both the energy contribute mutually, it is important to know their working limits. Through preliminary experimentation, it was found that temperature on the barrel surface less than 280 °C has increased the load on the motor to rotate the screw. This is because the viscosity of the material decreases with an increase in temperature, which allows the screw to freely rotate and compress the material. Hence based on the phenomenon minimum temperature at this region has been set as 290 °C with an increase of 12.5 °C for every set of extrusion temperature.

3.3.1.3   Metering zone

Usually, this zone has to be at a higher temperature to make sure that any material left behind needs to reach the fluidic state to travel out of the nozzle. If temperature is not accurately maintained, the pressure built up near the nozzle exit would not be sufficient to push the material out. Apart from this, it is also important to maintain the material in semi fluidic state for a limited period (approximately 10 seconds) to allow it to deposit and take shape before it rapidly cools down and solidifies. Hence based on the mentioned requirements, a minimum temperature of 320 °C with an increment of 10 °C for each set has been provided.

With the range for each zone, experiments have been conducted to study the mechanical characteristics of the extruded sample. Table 3-2 shows different sets of extrusion temperatures used for each iteration with variation in temperatures along zones, as mentioned previously.

Table 3-2 Extrusion temperature for different experiments

Experiments\ Zones	Feeding	Compression	Metering
Set-1	220 °C	290 °C	320 °C
Set-2	235 °C	302.5 °C	330 °C
Set-3	250 °C	315 °C	340 °C
Set-4	265 °C	327.5 °C	350 °C
Set-5	280 °C	340 °C	360 °C

Extrusion was repeated for each Set temperature as discussed previously, and samples were collected for every 5 minutes of extrusion after the extrusion process has reached a steady state. Figure 3-5 shows sampled collected after extrusion for set-1, set-2 and set-3.

29
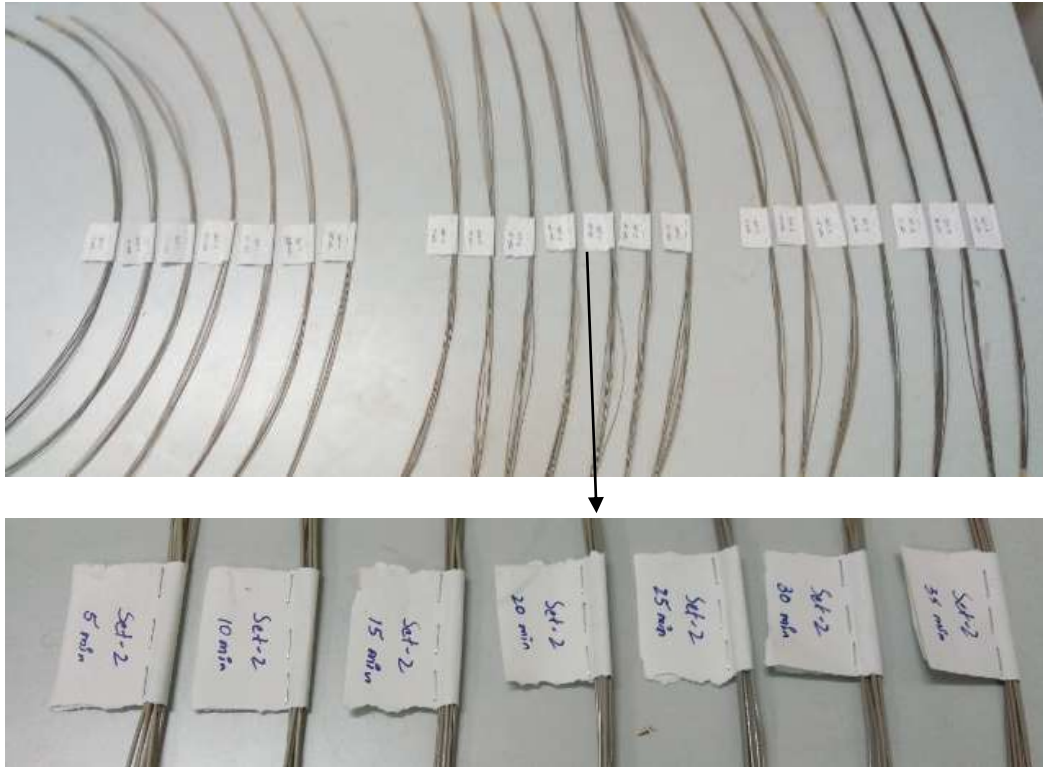
Figure 3-5 Wire samples for different extrusion temperature

3.4 Multi-pass sample preparation

Tensile specimens were made by depositing extruded filament onto X-Y moving table. Simple area filling geometry has been considered to make a rectangular specimen of size 75 mm by 20mm with variable deposition speeds. Variable speeds for XY Table was provided to accommodate excessive material deposition at the corners. Following are the process parameters taken into consideration to generate samples

1. Nozzle size
2. Extrusion temperature
3. Print Direction
4. Road Width
5. Standoff distance

3.4.1 Nozzle size

Nozzle size plays an important role in deciding the accuracy and speed of depositions. Usually smaller nozzle size ensures better accuracy of the specimen but at the cost of higher build time. Nozzle sizes corresponding to 0.7mm diameter, 1.1mm diameter and 1.5mm diameter have experimented. Fig 3-6 shows samples deposited with different nozzle diameters.
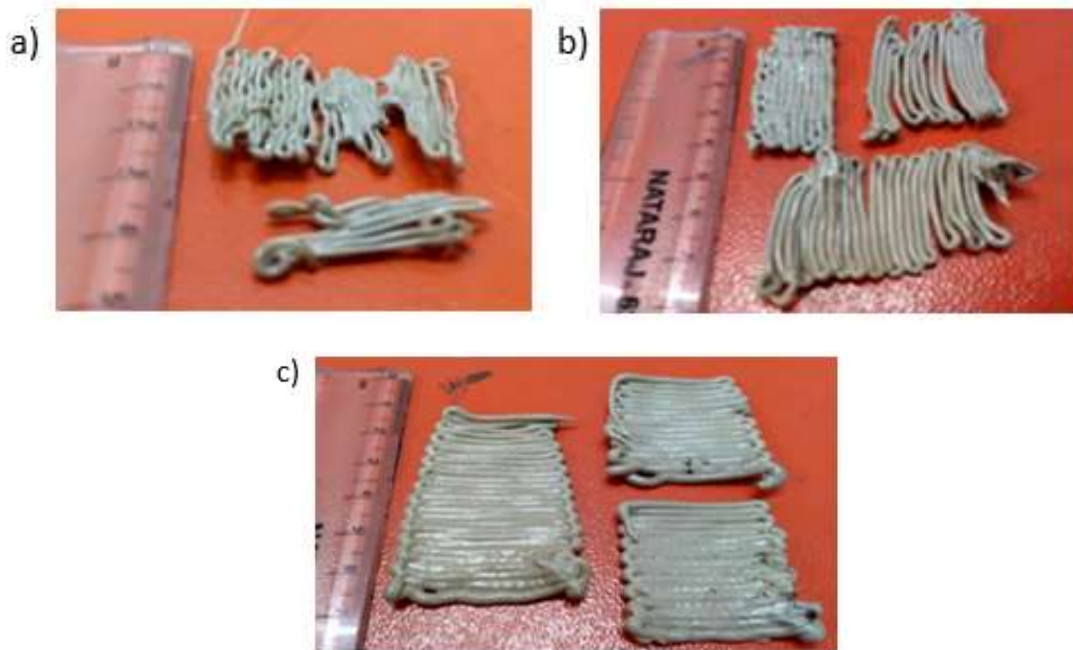
Figure 3-6 Samples Deposited with different nozzle diameters

a) 0.7mm b) 1.1mm c) 1.5mm

Preliminary experimental findings indicate that when using nozzle sizes below 1.5 mm due to its smaller opening for the material to move out the back pressure has increased which resulted in more load on the motor for operation. This has caused more vibrations, which resulted in inaccurate depositions of samples.

3.4.2   Extrusion temperature

From preliminary experiments, it was clear that the extrusion temperature corresponding to set-3 has shown better mechanical properties among all. Hence, this set along with adjoining sets corresponding to slightly higher and lower temperatures was selected. To avoid any confusion with the wire samples, these sets will be henceforth referred as Set-A, Set-B, Set-C. Table 3-3 shows the extrusion temperatures used during the deposition process.

Table 3-3 Extrusion temperatures for tensile specimen

Temperature at zones	Feeding	Compression	Metering
Set-A	235 °C	302.5 °C	330 °C
Set-B	250 °C	315 °C	340 °C
Set-C	265 °C	328.5 °C	350 °C

3.4.3   Print Direction

Print direction refers to depositing specimen in a particular orientation. Due to the complexity of the deposition process only print direction of 90 ° has been selected over 0°. Based on 90 ° print direction the parameter that can be investigated include bond strength. Fig 3-7 shows samples deposited with different print directions
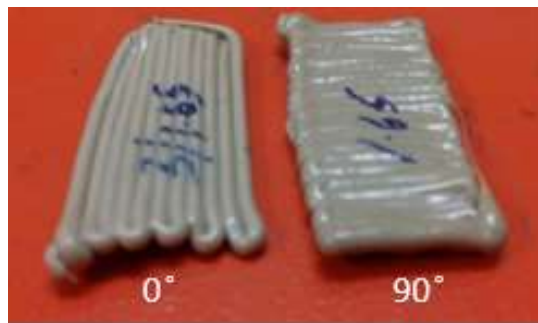
Figure 3-7 Samples deposited with 0 ° and 90° print direction

3.4.4   Road Width

Road width refers to the distance between two neighbouring passes in a plane. Figure 3-8 shows specimens deposited with different road gap. Road width is one of the critical factors in determining the bond strength between passes. Larger road width leads to the minimal cross-sectional area of contact between two passes, which results in week strength of the bond. On the other hand, smaller road width creates nonlinear deposition between layers causing the uneven surface of the specimen. Since we are extruding filament using 1.5mm diameter nozzle, considering the effects of die swelling along with experimentation the minimum road gap that was chosen was 1.6mm, and the maximum was 1.65mm after which there was minimum contact area between two passes. Table 3-4 shows a summary of road width parameters used in the experimentation.

32

Table 3-4 Experimental settings for road width

Levels		
1	2	3
1.6mm (1.06D)	1.65mm (1.1D)	1.7mm (1.13D)

Figure 3-8 Specimens deposited with different road gap

3.4.5   Standoff Distance

Standoff distance refers to the distance between the tip of the nozzle to the deposition surface. Figure 3-9 shows the sample being printed with standoff distance of 3mm.

Figure 3-9 Sample being printed with a standoff distance of 3mm

Experimentally it was found that lower standoff distance has resulted in better accuracy of the specimen, hence minimum stand of distance of 3mm which include 1mm for clearance was maintained to avoid material agglomeration near the nozzle end.

3.5   Design of Experiments

Table 3-5 shows a summary of the process parameters that have been used to conduct experiments. Full factorial design framework has been used to conduct the experiments. Since the number of factors is 2 out of which one factor has got 3 level and other with two levels the total number of experimental combinations, including $2^1 * 3^1$ which is 6. List of parameters with levels for the experimental study has been discussed in Fig 3-10 and Table 3-6.

Table 3-5 Summary of parameters and levels for experiments

Parameters	Levels		
	1	2	3
Print Direction	90°		
Road gap	1.06D (1.6 mm)	1.1D (1.65 mm)	
Stand off distance	2D (3mm)		
Extrusion temperature	330 °C (Set-A)	340 °C (Set-B)	350 °C (Set-C)
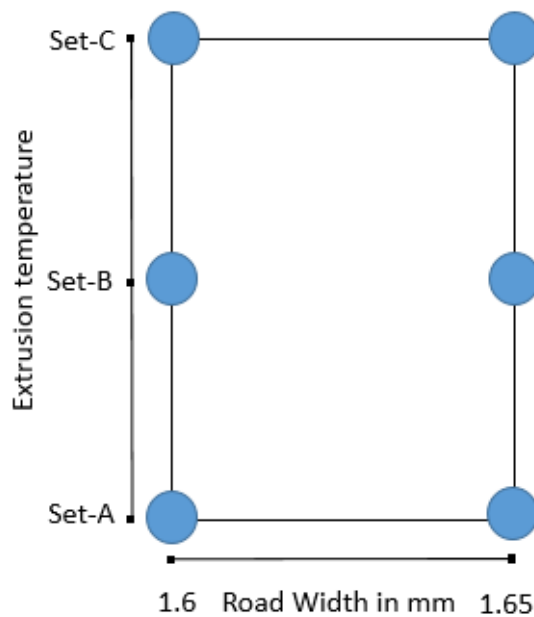
Figure 3-10 Pictorial view of experimental design

Table 3-6 Experimental settings

Experiments	Print Direction (P_D)	Extrusion temperature (T_E)	Road Width (W)	Bond Strength
		° C	mm	MPa
1	90 °	330 (Set-A)	1.06D	
2	90 °	330 (Set-A)	1.06D	
3	90 °	340 (Set-B)	1.06D	
4	90 °	340 (Set-B)	1.1D	
5	90 °	350 (Set-C)	1.1D	
6	90 °	350 (Set-C)	1.1D	

CHAPTER-4

Experimental Results

4.1 Tensile testing of wire samples

Tensile testing of wire samples has been performed using a numerical system equipped with a load cell. The standard gauge length of 100 mm was chosen based on axis movement constraints. One end of the spindle has been attached to the load cell while the other end is free to move. The wire has been firmly wounded and tightened in the provision attached to the spindles. For each extrusion temperature set and time combination, tensile tests were repeated thrice. Figure 4-1 shows the experimental setup used for wire testing.

Figure 4-1 Wire testing setup

4.1.1 Set-1 [220 ° C, 290 ° C, 320 ° C]

It has been observed that the ultimate tensile strength for extruded samples after 20 minutes of continuous extrusion has shown ultimate tensile strength of 75.6 MPa while that of 5 minutes and 35 minutes showed ultimate tensile strength of 72.8 MPa and 74.6 MPa respectively. Stress-strain plots for samples with Set-1 temperature settings are shown in Figure 4-2.
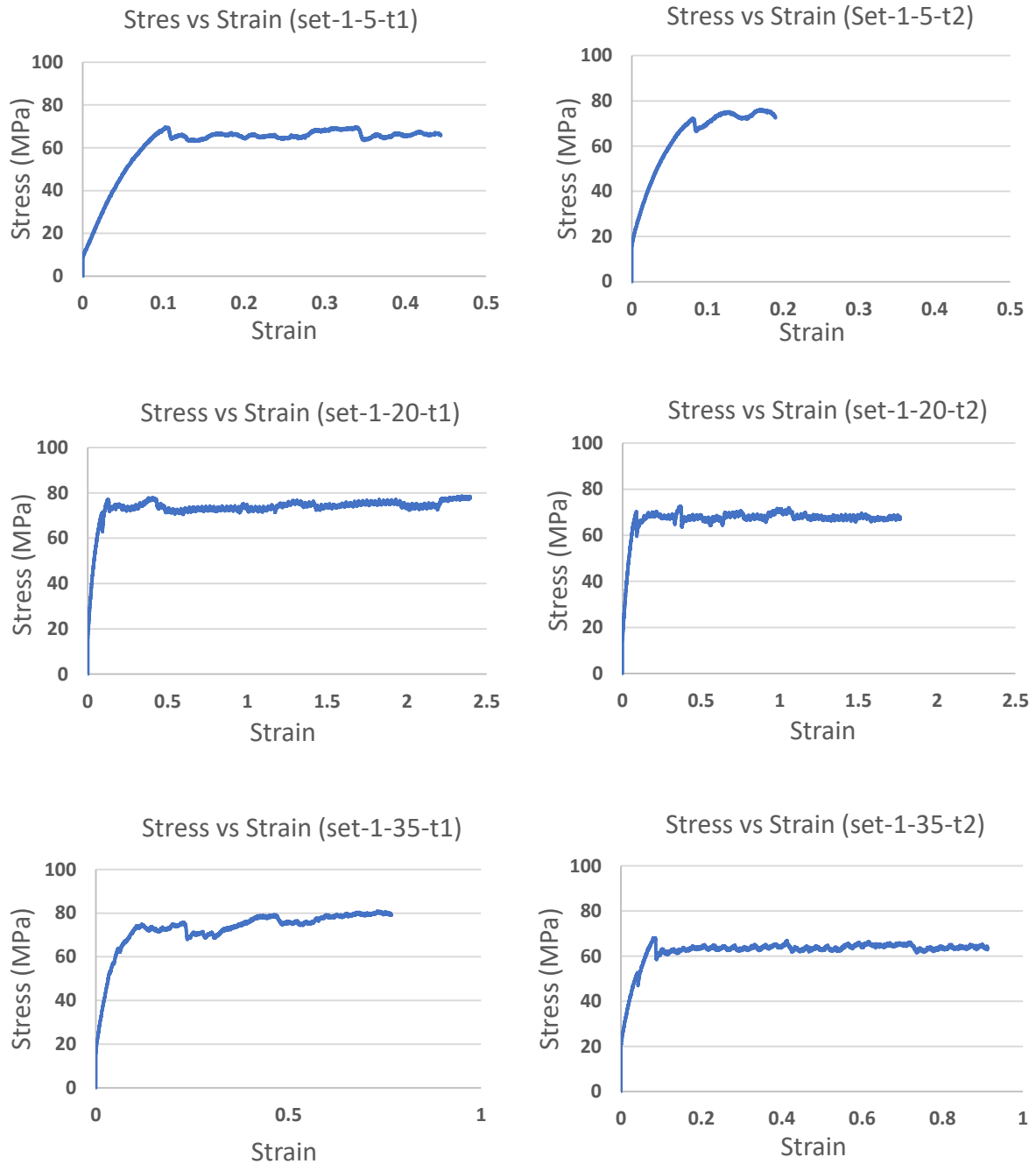
Figure 4-2 Stress-strain plots for set-1 extrusion temperature wire samples

4.1.2   Set-2 [235 °C, 302.5 °C, 330 °C]

Wire samples corresponding to set -2 have resulted in more consistent results with less variation for each test sample as compared to set-1. The ultimate tensile strength of set-2 was highest for 35 minutes of continuous extrusion whose magnitude was 80.18 MPa followed by 77.68 MPa and 74.57 MPa for 5 minutes and 20 minutes respectively. Figure 4-3 shows stress-strain plots for set-2 extrusion temperature with different extrusion time after the steady state temperature has reached.

37
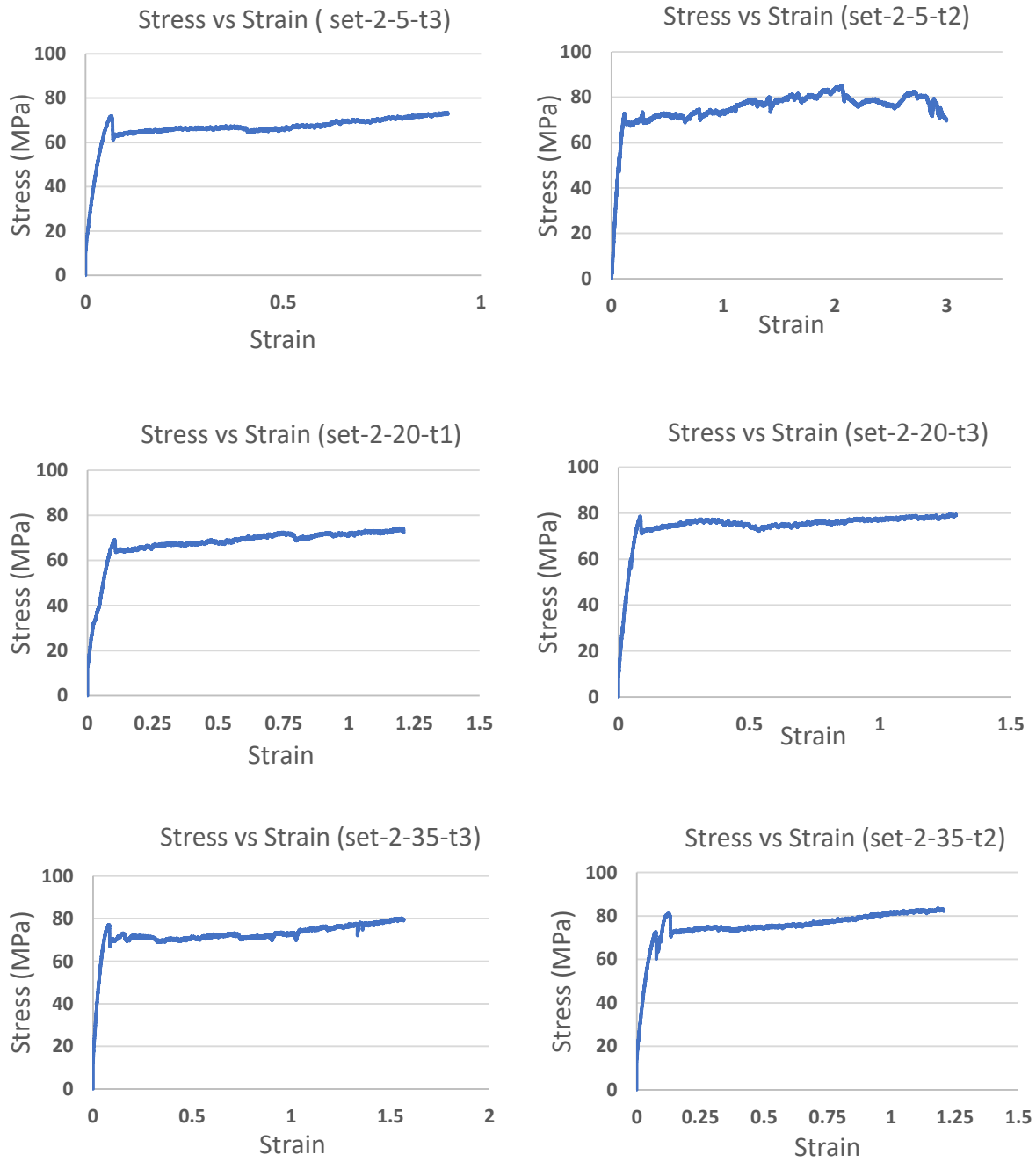
Figure 4-3 Stress-strain curve for set-2 extrusion temperature wire samples

4.1.3 Set-3 [250 °C, 315 °C, 340 °C]

Among all set-3 extrusion temperature have resulted in higher tensile strength with a maximum of 83.7 MPa for 5 minutes and 35 minutes of extrusion, as shown in Figure 4-4. The minimum strength which was recorded] as 78 MPa corresponding for 20 minutes of extrusion.
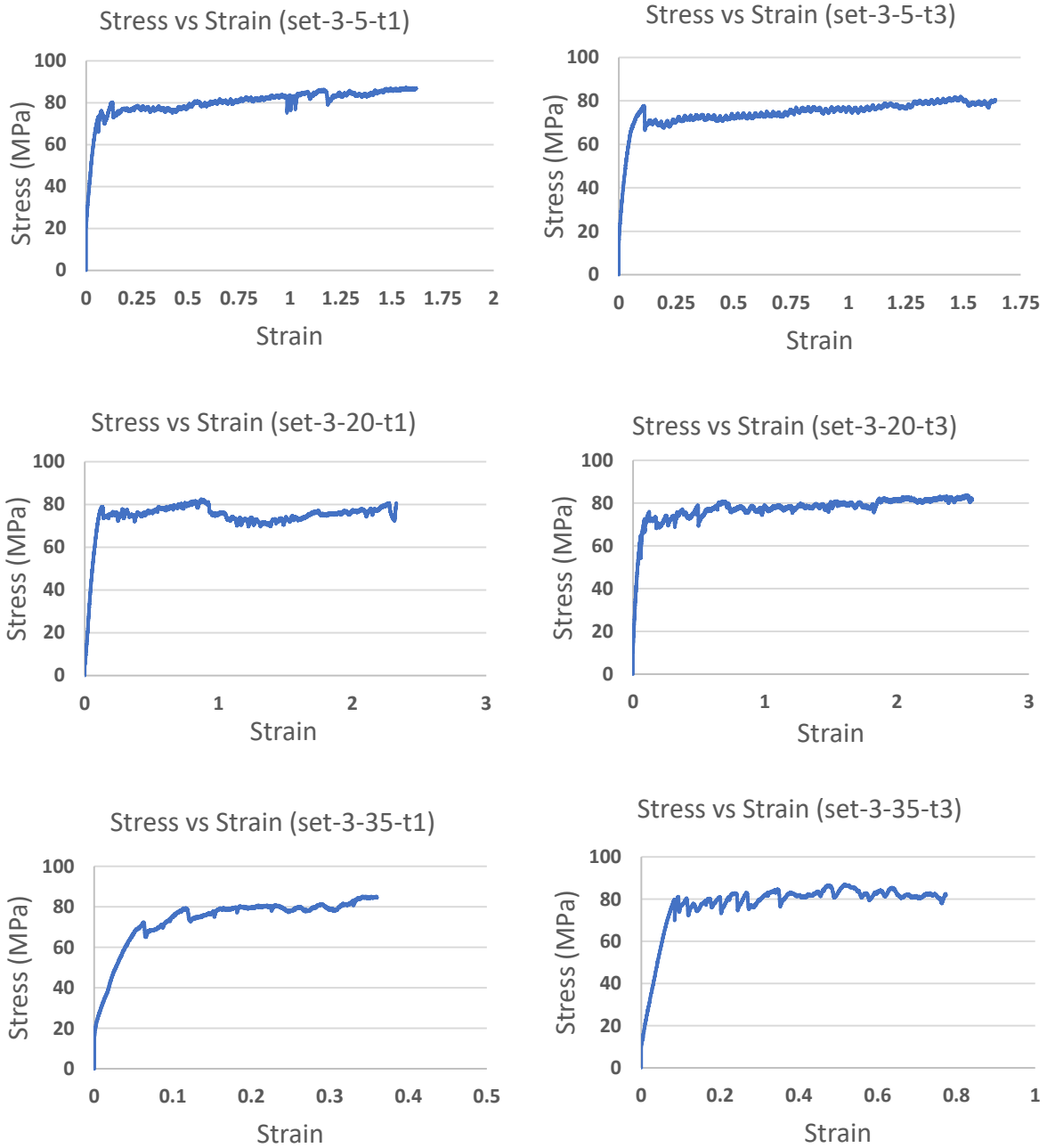
Figure 4-4 Stress-strain curve for set-3 extrusion temperature wire samples

4.1.4 Set-4 [265 °C, 327.5 °C, 350 °C]

As shown in Figure 4-5, the ultimate tensile strength has reduced in set-4 extrusion setting. The strength slowly reduced to 77.7 MPa and 74.4 MPa for 20 minutes and 35 minutes, respectively. This decreasing strength pattern might be due to material degradation thereby losing its properties.
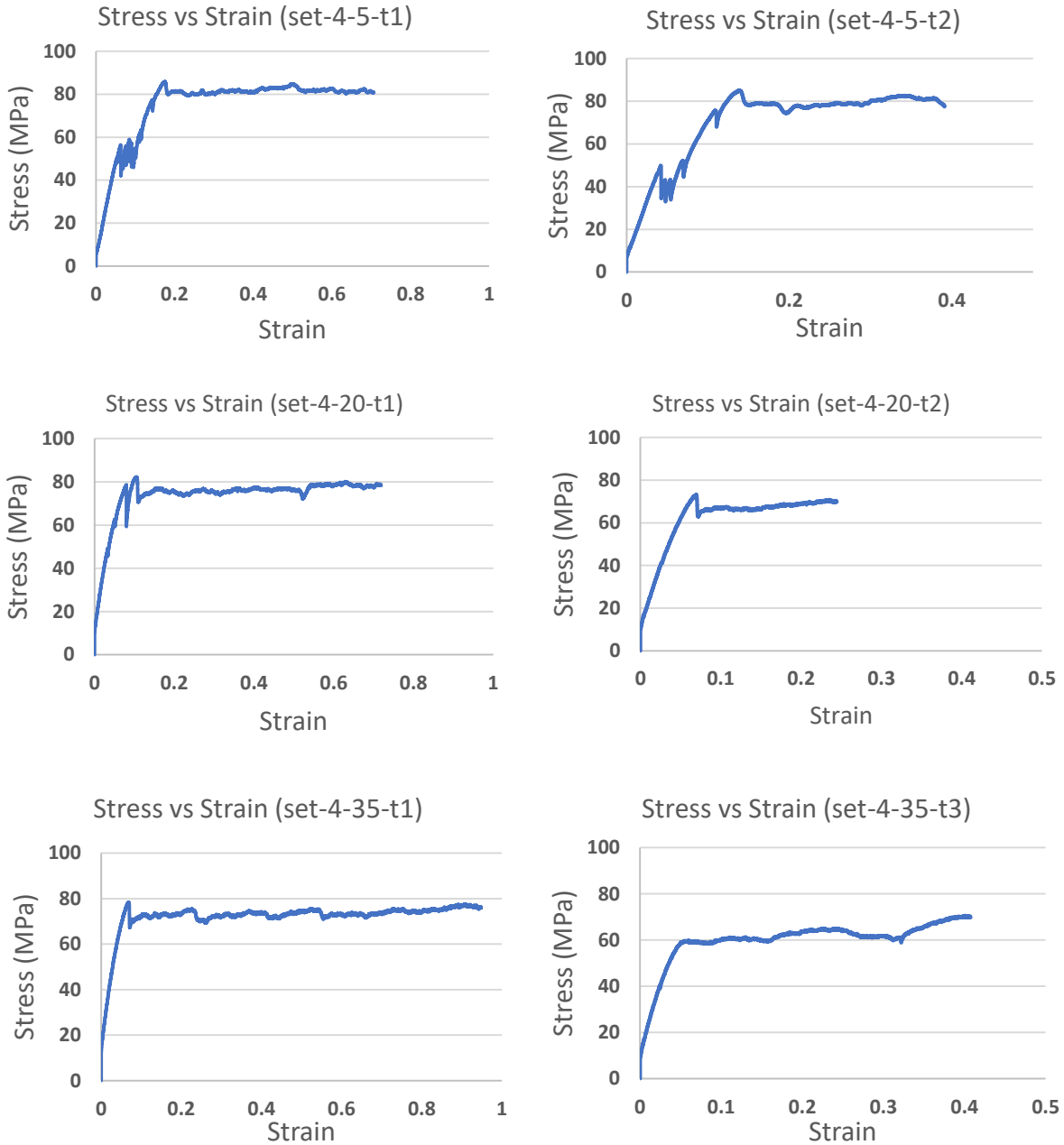
Figure 4-5 Stress-strain curve for set-4 extrusion temperature wire samples

4.1.5 Set-5 [280 °C, 340 °C, 360 °C]

It can be observed from plots shown in Figure 4-6 that the tensile strength results of set-5, when compared to set-4 extrusion temperatures, are further lower which suggests that material degradation is more significant with a much lower tensile strength of 68.4 MPa for 5 minutes
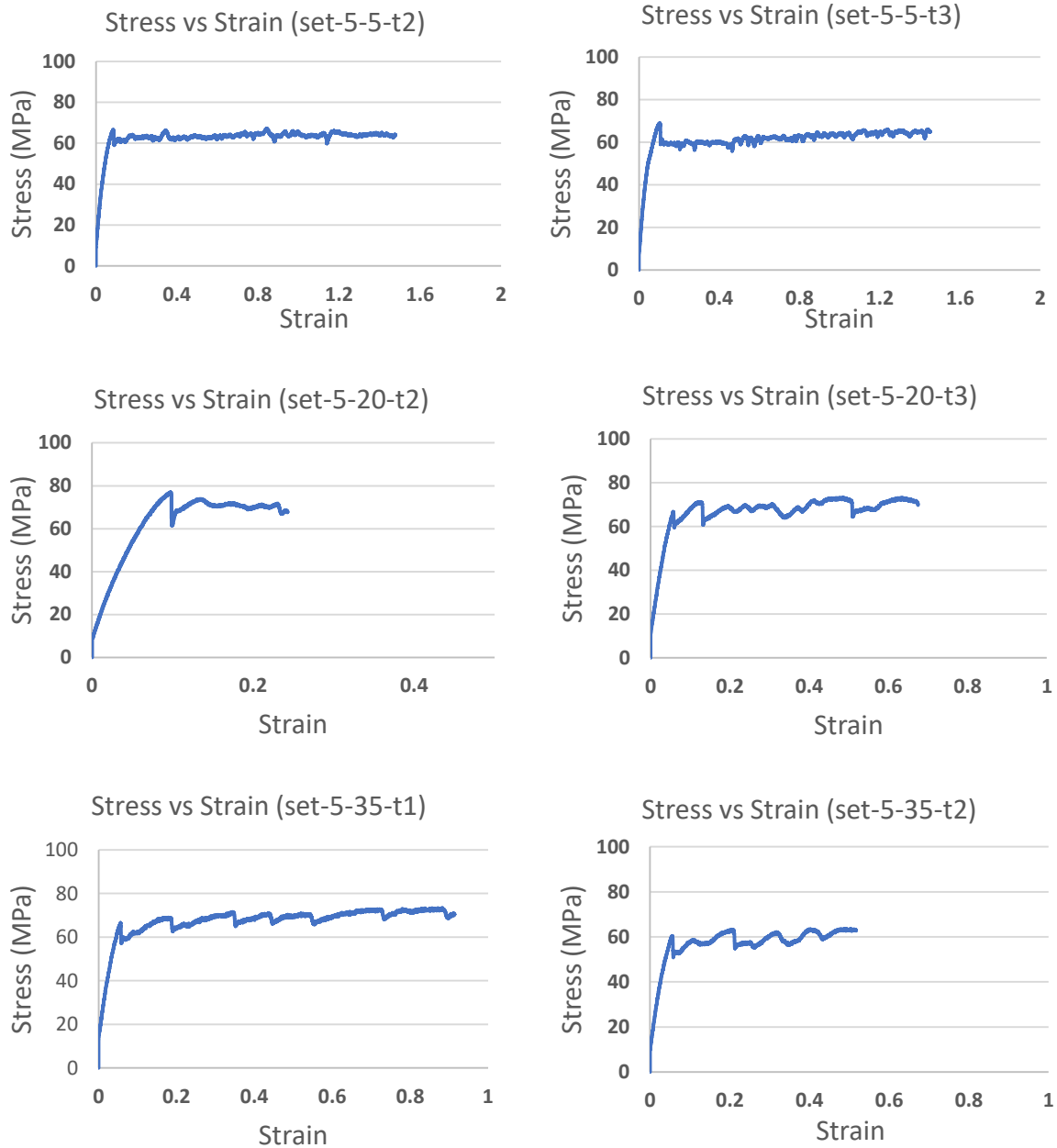
Figure 4-6 Stress-strain curve for set-5 extrusion temperature wire samples

It was clear from results that after set-3 extrusion temperature, the magnitude of ultimate tensile strength had seen a falling trend. This is because excessive extrusion temperature has overheated the polymer resulting in material degradation. Also, one can notice from the results that samples of set-4 and set-5 have undergone less elongation which indicates that the material has failed in a manner similar to brittle failure due to material degradation caused by overheating.
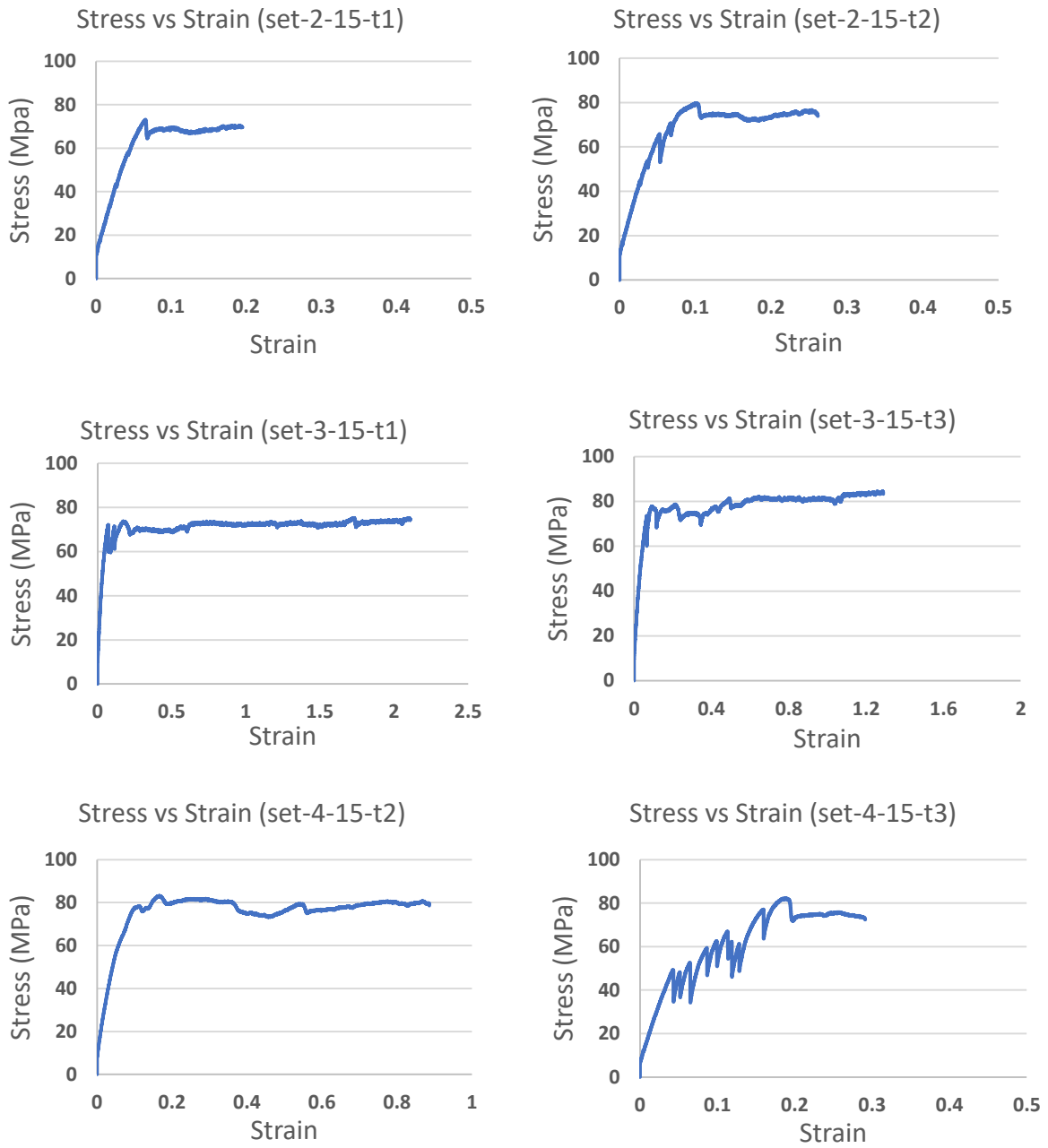
Figure 4-7 Stress-strain curve for 15 minutes of extrusion for set-2, set-3 and set-4 temperature setting

With an overview of results that set-2 set-3 and set-4 extrusion temperature provided necessary information through consistent results further test was performed for 15 minutes and 25 minutes of extrusion time as shown in Figure 4-7 and Figure 4-8 respectively.
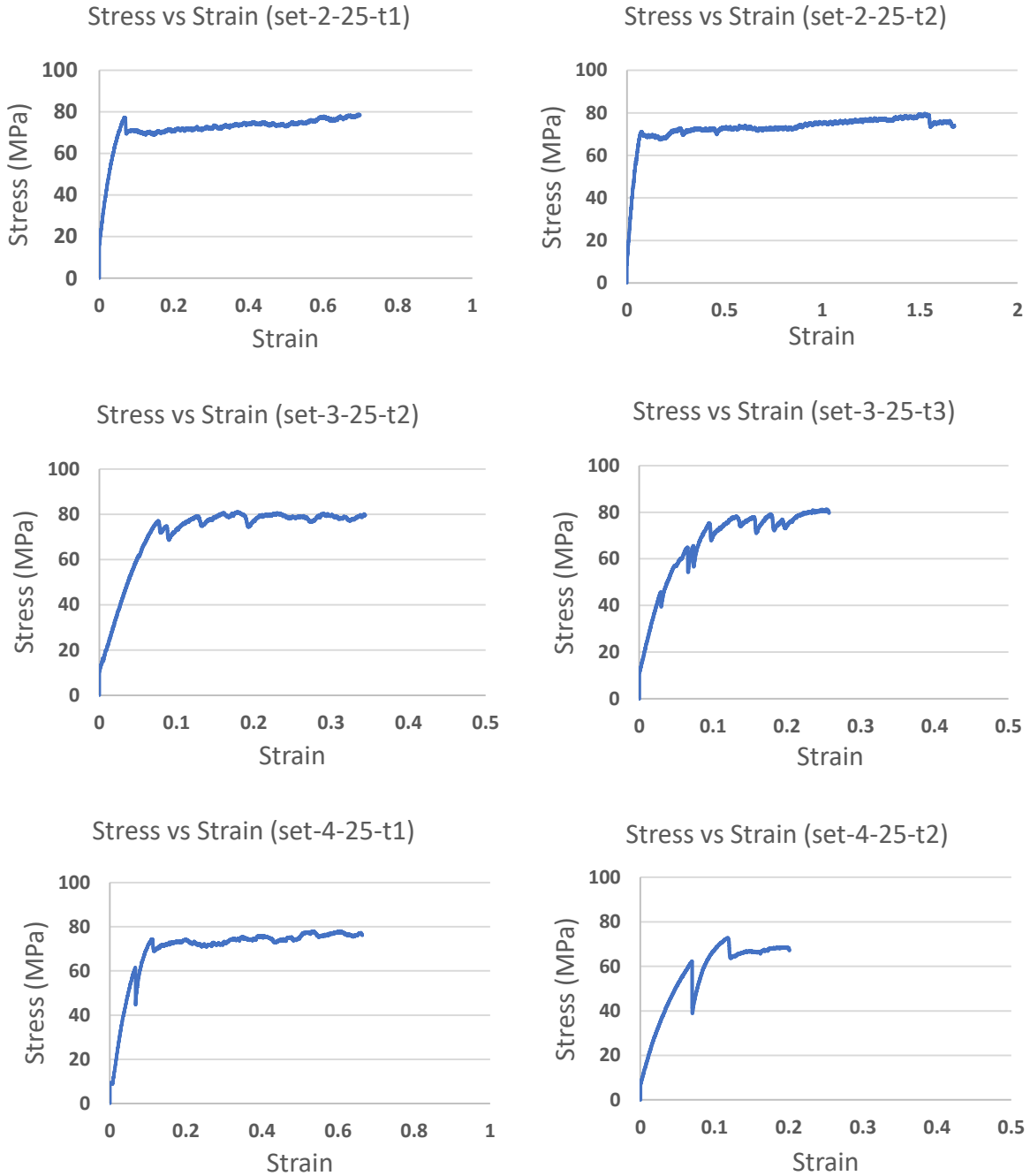
Figure 4-8 Stress-strain curve for 15 minutes of extrusion for set-2, set-3 and set-4 temperature setting

4.1.6   Summary of wire testing results

All the previously discussed tensile results of wire samples have been summaries in Figure 4-9 and Table 4-1. It can be observed that among all the extrusion temperatures set-3 temperature setting has yielded higher tensile strength of 83.7 MPa. Trend pattern suggests a gradual decrease in the tensile strength of samples after set-3 extrusion temperature caused

due to material degradation accompanied by higher extrusion temperature, hence set-3 temperature setting was considered favourable for extrusion.

Table 4-1 Results summary of wire testing for different extrusion temperatures

Set-time	Test-1	Test-2	Average	Minutes	Ultimate Tensile Strength (MPa)
set-2-5	70.01	85.34	77.68	5	77.68
set-3-5	87.35	80.07	83.71	5	83.71
set-4-5	85.93	85.08	85.50	5	85.50
set-2-15	73.10	79.78	76.44	15	76.44
set-3-15	75.31	84.68	80.00	15	80.00
set-4-15	83.20	82.25	82.72	15	82.72
set-2-20	74.35	74.79	74.57	20	74.57
set-3-20	82.59	74.88	78.74	20	78.74
set-4-20	82.33	73.20	77.77	20	77.77
set-2-25	78.92	79.71	79.31	25	79.31
set-3-25	81.02	81.24	81.13	25	81.13
set-4-25	78.10	72.94	75.52	25	75.52
set-2-35	76.80	83.56	80.18	35	80.18
set-3-35	85.23	82.15	83.69	35	83.69
set-4-35	78.37	70.53	74.45	35	74.45

Ultimate Tensile Strength vs Time for different Extrsuion temperatures
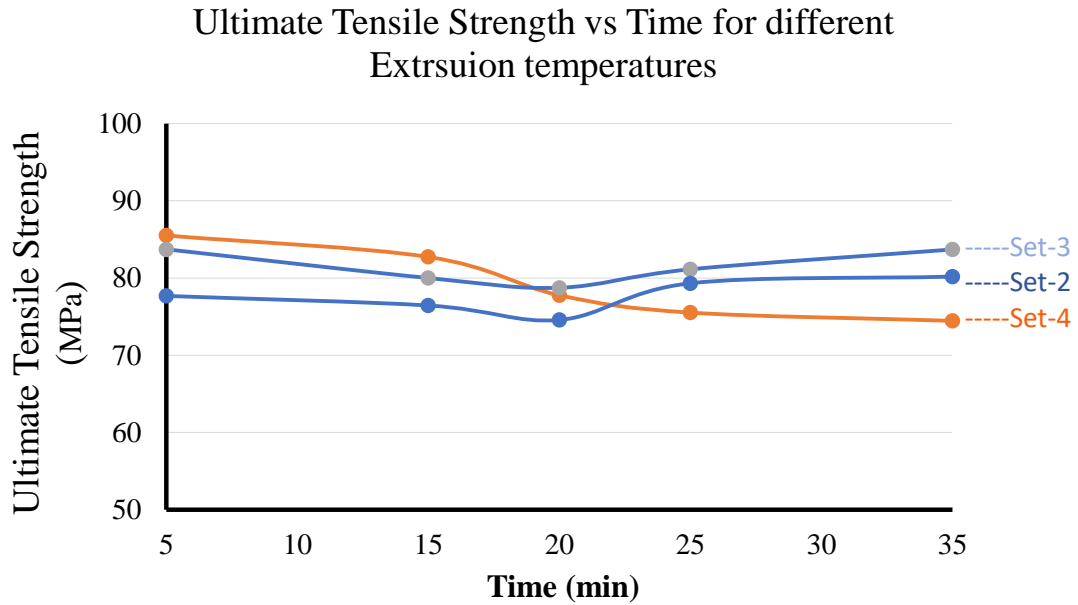
Figure 4-9 Summary of wire testing results for different extrusion temperatures

4.2 Tensile testing of multi-pass specimen

Tensile tests have been performed on deposited specimens to study the behaviour of bond strength. Figure 4-10 shows a sample being tested with UTM. The samples being investigated have been set with standard gauge length 18mm and gripping length of 28mm on each side.

Figure 4-10 PEEK specimen testing with UTM

Samples have been fabricated with varying road width and extrusion temperatures as process parameters. All the samples have been deposited perpendicular to the loading direction, which resulted in obtaining inter road strength as the response variable.

4.2.1   Set-A [235 °C, 302.5 °C, 330 °C] with different road width

Results indicate that road gap played an important role in deciding the interbond strength. It can be visualized that as the road gap increases the net cross section area of contact decreases, which leads to failure in the sample at lower stress levels. As shown in Figure 4-11 for similar extrusion temperature, the effect on interbond strength for 1.6mm and 1.65mm road width has changed from 53.43 MPa to 47.66 MPa.

Figure 4-11 Stress-strain behaviour for different road widths corresponding to Set-A extrusion temperature

4.2.2   Set-B [250 °C, 315 °C, 340 °C] with different road width

While the effect of road width is similar to that of the previous experimental results, Set-B extrusion temperature with lower road width has resulted in maximum inter road strength among all. It can also be observed that due to the sufficient temperature the deposited

46

material gained enough time to properly bond with the previously pass which was also reflected by lesser variation in bond strength as a comparison to the previous experiments. Figure 4-12 shows stress-strain plots for set-3 extrusion temperature with different road width.
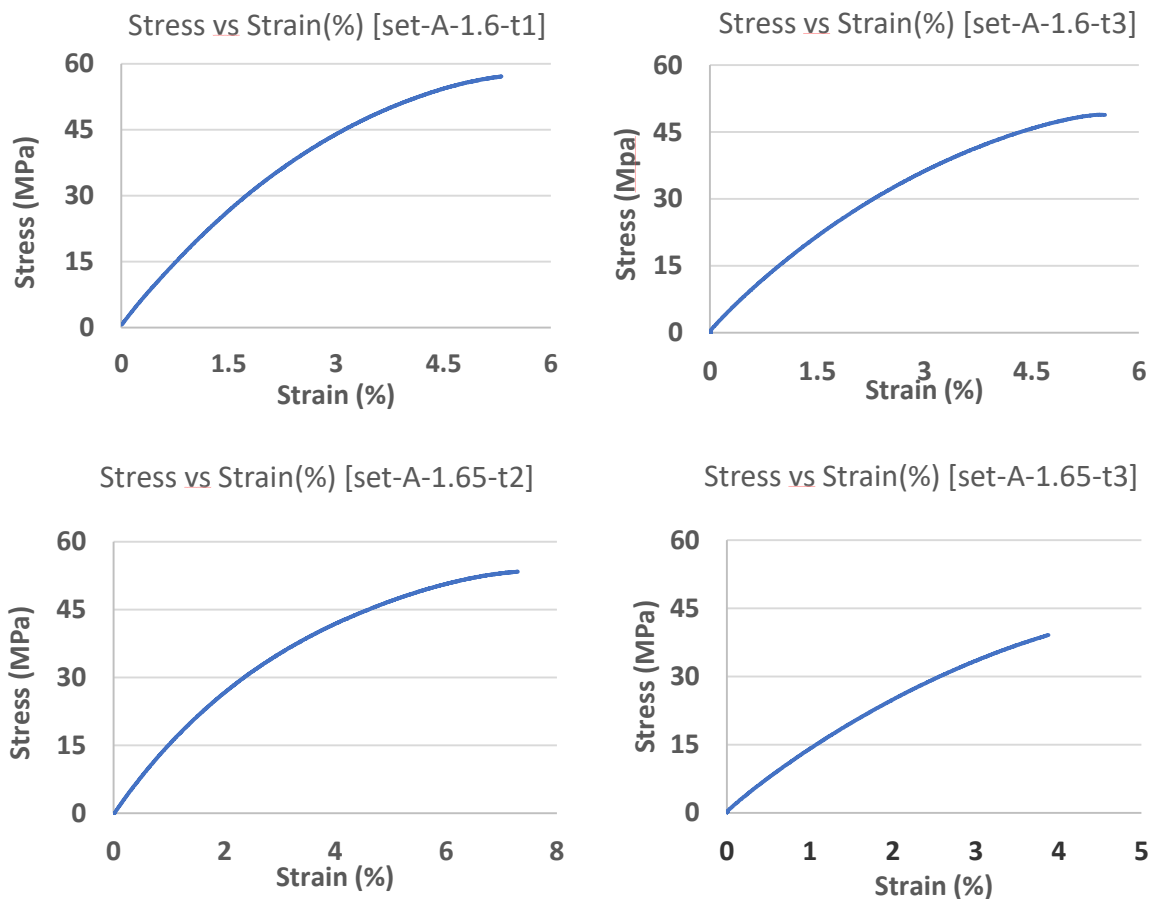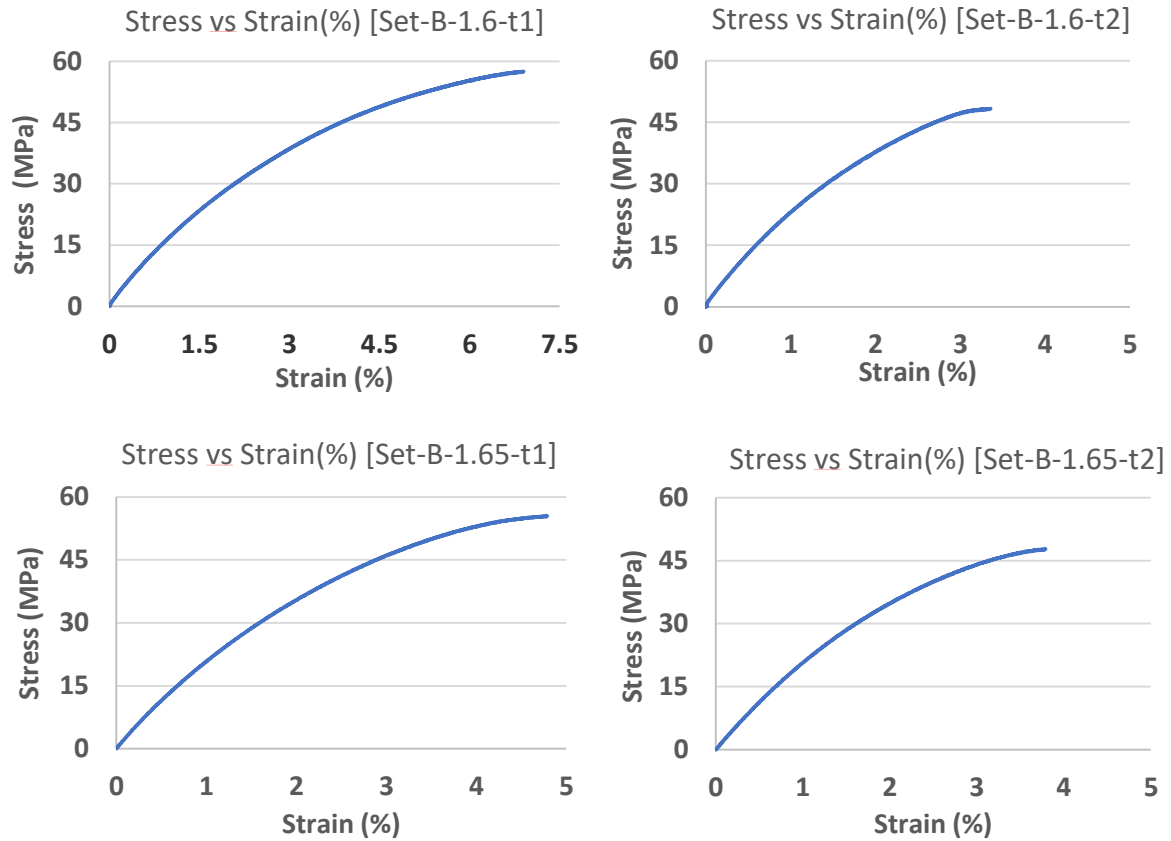

Figure 4-12 Stress-strain behaviour for different road widths corresponding to Set-B extrusion temperature

4.2.3 Set-C [265 °C, 327.5 °C, 350 °C] with different road width

It can be observed from the results, as shown in Figure 4-13 that higher extrusion temperature has affected the interbond strength in a similar fashion as that of wire testing. Among all the tensile samples, the Set-C temperature extruded samples have recorded the least bond strength. This is caused due to excessive heating, which resulted in material degradation. It was interesting to note that variation in bond strength has decreased as compared to the previous tests, which indicates that as extrusion temperature is increased the effect of material degradation is more prominent than road width.
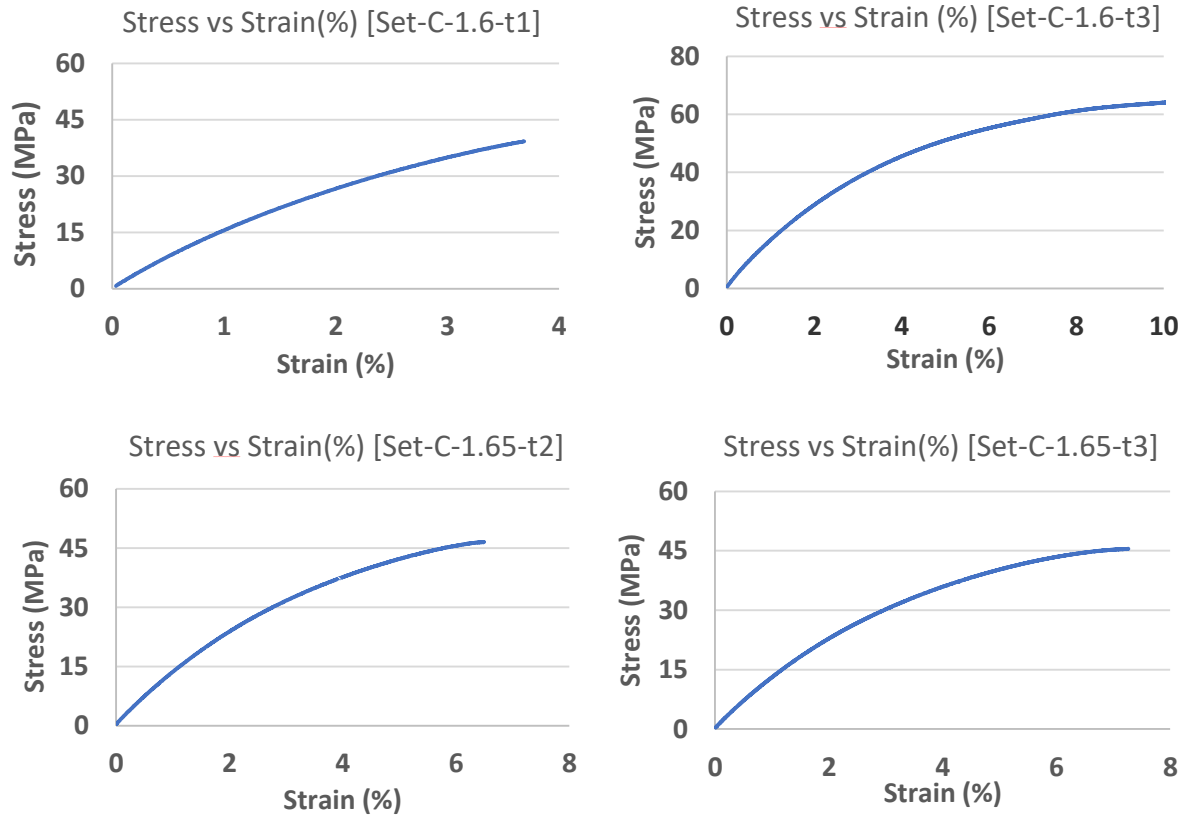
Figure 4-13 Stress-strain behaviour for different road widths corresponding to Set-C extrusion temperature

4.2.4   Summary of tensile testing results for multi-pass sample

Results indicate that road width has a significant contribution in deciding the interbond strength. Table 4-2 and Figure 4-14 shows a summary of tensile testing results.

Table 4-2 Summary of Bond strength results for different parameters

Extrusion Temperature °C	Road width (mm)	Maximum bond strength (MPa)			
		Test-1	Test-2	Test-3	Average
Set-A	1.6	57.1	54.3	48.9	53.43
	1.65	50.5	53.4	39.1	47.66
Set-B	1.6	57.4	48.3	56.96	54.22
	1.65	55.47	47.77	47.78	50.34
Set-C	1.6	39.94	45.24	64.21	49.79
	1.65	46.08	46.57	45.49	46.04

48
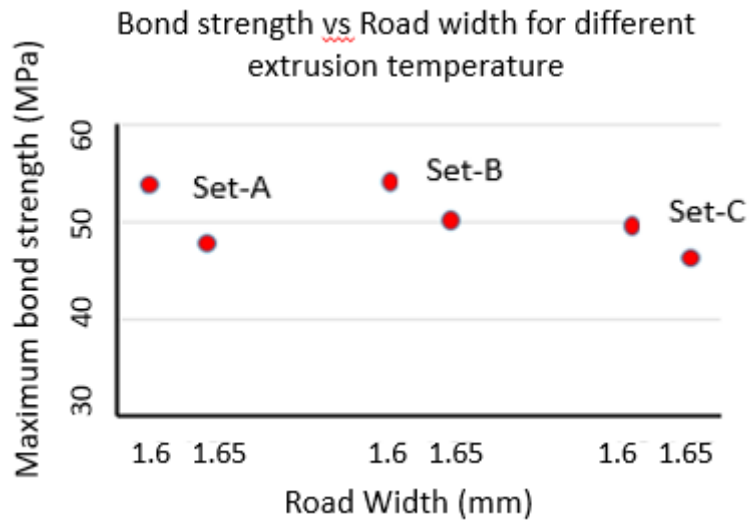
Figure 4-14 Bond strength variation for different parameter settings

It was observed that lower road width has contributed to higher interbond strength. This was because lower road width causes the material to deposit closely which results in higher contact area between two passes.

4.3 Summary

Experimental results indicate that material extruded with extrusion temperature beyond 350 °C has resulted in material degradation. Study on other process parameters suggested that lower standoff distance and road width yield in higher inter road strength. It was also observed that the effect of road width is suppressed by extrusion temperature when processing material at higher temperatures.

CHAPTER -5

Conclusion and Future scope

5.1   Conclusion

In the present work, an analytical study has been conducted on screw extrusion of PEEK along with experimental work to determine the effect of various process parameters like extrusion temperature, bed temperature, road width and standoff distance on mechanical behaviour by fabricating wire samples and tensile samples. Following are the key observations resulting from the experiments.

1. From tensile testing of wire samples, it was observed that extrusion temperature lower than 350 °C of nozzle temperature has resulted in higher tensile strength. Samples collected by extruding with nozzle temperature beyond 350 °C have undergone material degradation due to excessive heating. The material degradation has also been reflected in the strain behaviour of samples with less elongation compared to other lower extruded temperature samples.

2. Through the experimental study, it was clear that lower standoff distance has reflected in better geometrical accuracy of the components; hence minimum stand of distance was maintained during tensile specimen deposition. Tensile testing results of samples with different parameter setting indicated that road width plays an important role in deciding the inter road strength. Samples made with higher road width have shown lower bond strength due to small area overlap, which reduces the net cross section. It was also noted that the effect of road width is suppressed with an increase in extrusion temperature, which indicates that the material degradation effect is more prominent than road width at higher extrusion temperatures. Within the working range of road width and extrusion temperature lower road width with a nozzle temperature below 350 °C has resulted in maximum inter road strength.

5.2   Future scope

The following are the considerations for future scope

1. The current experimental study was focused only on single layer depositions and understanding of multi-layer needs to evolve.

2. All the deposition performed were restricted to $90\,^\circ$ print direction due to warping effect when making samples with a larger dimension. This effect can possibly be eliminated by using a heated bed in order to maintain the necessary thermal gradients.

3. The material feeding, although being continuous, is not consistent in delivering material into the extruder; this causes air entrapments in the extruded filament as well as inconsistency in the material flow output. This effect can be minimized by varying the motor rpm by using a rheostat and synchronising the rpm of the motor according to the flow rate.

4. The XY table that has been used for depositing tensile samples is offered only with the X axis and Y axis movement, but it can be expanded to Z-axis movement through auxiliary attachment to deposit layers one above the other and form a wide range of components.

References

[1] Joshi, S.C. and Sheikh, A.A., 2015. 3D printing in aerospace and its long-term sustainability.Virtual and Physical Prototyping, 10(4), pp.175-185.

[2] Novakova-Marcincinova, L., Novak-Marcincin, J., Barna, J. and Torok, J., 2012, June. Special materials used in FDM rapid prototyping technology application. In 2012 IEEE 16th International Conference on Intelligent Engineering Systems (INES) (pp. 73-76). IEEE.

[3] Victrex, P.E.E.K., 2015. Material properties guide.

[4] Natti S.. Rao and Keith T.. O'Brien, 1998. Design Data for Plastics Engineers. Hanser publishers.

[5] Baird, D.G. and Collias, D.I., 2014. Polymer processing: principles and design. John Wiley & Sons.

[6] Rinaldi, M., Ghidini, T., Cecchini, F., Brandao, A. and Nanni, F., 2018. Additive layer manufacturing of poly (ether ether ketone) via FDM. Composites Part B: Engineering, 145, pp.162-172.

[7] Deng, X., Zeng, Z., Peng, B., Yan, S. and Ke, W., 2018. Mechanical properties optimization of poly-ether-ether-ketone via fused deposition modelling. Materials, 11(2), p.216.

[8] Xiaoyong, S., Liangcheng, C., Honglin, M., Peng, G., Zhanwei, B. and Cheng, L., 2017, January. Experimental analysis of high temperature PEEK materials on 3D printing test. In 2017 9th International Conference on Measuring Technology and Mechatronics Automation (ICMTMA) (pp. 13-16).

[9] Wenzheng, W., Geng, P., Li, G., Zhao, D., Zhang, H. and Zhao, J., 2015. Influence of

layer thickness and raster angle on the mechanical properties of 3D-printed PEEK and a comparative mechanical study between PEEK and ABS. Materials, 8(9), pp.5834-5846.

[10] Yang, C., Tian, X., Li, D., Cao, Y., Zhao, F. and Shi, C., 2017. Influence of thermal processing conditions in 3D printing on the crystallinity and mechanical properties of PEEK material. Journal of Materials Processing Technology, 248, pp.1-7.

[11] Tan, S., Su, A., Luo, J. and Zhou, E., 1999. Crystallization kinetics of poly (ether ether ketone)(PEEK) from its metastable melt. Polymer, 40(5), pp.1223-1231.

[12] Eduljee, R.F., Gillespie Jr, J.W. and McCullough, R.L., 1994. Residual stress development in neat poly (etheretherketone). Polymer Engineering & Science, 34(6), pp.500-506.

[13] Patel, P., Hull, T.R., McCabe, R.W., Flath, D., Grasmeder, J. and Percy, M., 2010. Mechanism of thermal decomposition of poly (ether ether ketone)(PEEK) from a review of decomposition studies. Polymer Degradation and Stability, 95(5), pp.709-718.

[14] Lu, S.X., Cebe, P. and Capel, M., 1996. Thermal stability and thermal expansion studies of PEEK and related polyimides. Polymer, 37(14), pp.2999-3009.

[15] Bellini, A., Shor, L. and Guceri, S.I., 2005. New developments in fused deposition modelling of ceramics. Rapid Prototyping Journal, 11(4), pp.214-220.

[16] Reddy, B.V., 2006. ''Extrusion deposition process for layered manufacturing.'' Masters of Technology - Thesis, Indian Institute of Technology Kanpur.

[17] Reddy, B.V., Reddy, N.V. and Ghosh, A., 2007. Fused deposition modelling using direct extrusion. Virtual and Physical Prototyping, 2(1), pp.51-60.

[18] Drotman, D.T., 2015. Design of a Screw Extruder for Additive Manufacturing (Doctoral dissertation, UC San Diego).

[19] Tseng, J.W., Liu, C.Y., Yen, Y.K., Belkner, J., Bremicker, T., Liu, B.H., Sun, T.J. and Wang, A.B., 2018. Screw extrusion-based additive manufacturing of PEEK. Materials &

Design, 140, pp.209-221.

[20] Termoplasti, Z. and Modeliranje, N., 2013. Processing poly (ether etherketone) on a 3D printer for thermoplastic modelling. Mater. Tehnol, 47, pp.715-721.

[21] Whyman, S., Arif, K.M. and Potgieter, J., 2018. Design and development of an extrusion system for 3D printing biopolymer pellets. The International Journal of Advanced Manufacturing Technology, 96(9-12), pp.3417-3428.

[22] McLauchlin, A.R., Ghita, O.R. and Savage, L., 2014. Studies on the reprocessability of poly (ether ether ketone)(PEEK). Journal of Materials Processing Technology, 214(1), pp.75-80.

[23] Kuo, C.F.J. and Su, T.L., 2006. Optimization of multiple quality characteristics for polyether ether ketone injection molding process. Fibers and Polymers, 7(4), pp.404-413.

[24] Hsiung, C.M., Cakmak, M. and White, J.L., 1990. Crystallization phenomena in the injection molding of poly ether ether ketone and its influence on mechanical properties. Polymer Engineering & Science, 30(16), pp.967-980.

[25] Park, K. and Kim, Y.S., 2009. Effect of mold temperature on mechanical properties of an injection-molded part with microfeatures. Journal of Polymer Engineering, 29(1-3), pp.135-154.

[26] Groover, M.P., 2007. Fundamentals of modern manufacturing: materials processes, and systems. John Wiley & Sons.

[27] Montgomery, D.C., 2017. Design and analysis of experiments. John wiley & sons.

[28] Kiemele, M.J., Schmidt, S.R. and Berdine, R.J., 1997. Basic statistics: Tools for continuous improvement. Air academy press.